

See discussions, stats, and author profiles for this publication at: <https://www.researchgate.net/publication/330210234>

Flight Testing Data Set for Subscale GA Aircraft: 26%-scale Cub Crafters CC11-100 Sport Cub S2

Conference Paper · January 2019

DOI: 10.2514/6.2019-1616

CITATIONS

0

READS

42

3 authors:



[Or Dantsker](#)

University of Illinois, Urbana-Champaign

24 PUBLICATIONS 106 CITATIONS

SEE PROFILE



[Moiz Vahora](#)

University of Illinois, Urbana-Champaign

10 PUBLICATIONS 10 CITATIONS

SEE PROFILE



[Renato Mancuso](#)

Boston University

39 PUBLICATIONS 330 CITATIONS

SEE PROFILE

Some of the authors of this publication are also working on these related projects:



Neuroflight [View project](#)



Single Core Equivalence (SCE) Framework [View project](#)

Flight & Ground Testing Data Set for Subscale GA Aircraft: 26%-scale Cub Crafters CC11-100 Sport Cub S2

Or D. Dantsker *

Al Volo LLC, Urbana, IL 61801

Moiz Vahora[†]

University of Illinois, Urbana, IL 61801

Renato Mancuso[‡]

Boston University, Boston, MA 02215

This paper presents a data set for subscale general aviation aircraft, a 26%-scale Cub Crafters CC11-100 Sport Cub S2, which will be the first of a series of aircraft data sets that will be published online and freely available as part of the Unmanned Aerial Vehicle Database (UAVDB). The Unmanned Aerial Vehicle Database will be expanded to include many aircraft as they are tested as well as data from ground testing such as moment of inertia testing and data reduction techniques that can be used. also include additional details regarding the airframe, instrumentation, flight test plan, as well as related work.

Nomenclature

<i>AHRS</i>	= attitude and heading reference system	<i>m</i>	= aircraft mass
<i>DOF</i>	= degree of freedom	<i>p, q, r</i>	= roll, pitch and yaw rotation rates
<i>ESC</i>	= electronic speed controller	<i>S</i>	= wing area
<i>GPS</i>	= global positioning system	<i>u, v, w</i>	= body-fixed true velocity
<i>IMU</i>	= inertial measurement unit	<i>V</i>	= total speed
<i>PWM</i>	= pulse width modulation	<i>x, y, z</i>	= position in ENU coordinate system
<i>Re</i>	= Reynolds number	<i>α</i>	= angle-of-attack
<i>RC</i>	= radio control	<i>β</i>	= sideslip angle
<i>UAV</i>	= unmanned aerial vehicle	<i>φ, θ, ψ</i>	= roll, pitch and heading angles
<i>a_x, a_y, a_z</i>	= body-axis translational acceleration	<i>ρ</i>	= density of air
<i>c</i>	= wing mean chord		

* Aero-Mechanical Engineer. ordantsker@alvolo.us

† Graduate Researcher, Department of Aerospace Engineering, AIAA Student Member. mvahor2@illinois.edu

‡ Assistant Professor, Department of Computer Science. rmancuso@bu.edu

I. Introduction

In the past several years, there has been a major increase in the popularity of unmanned aerial vehicles (UAVs) for research, military, commercial, and civilian applications. Part of this uptrend in UAV use includes increase in the research related to them. There have been UAVs used to study aerodynamic qualities,^{1,2} especially in high angle-of-attack conditions.³⁻⁵ Others have been used as testbeds to develop new control algorithms.⁶⁻¹¹ Additionally, some unmanned aircraft are used as low-cost stand-ins for experiments that are too risky or costly to perform on their full scale counterparts.¹²⁻¹⁵ Yet other times, unmanned aircraft are developed to explore new aircraft configurations¹⁶⁻¹⁹ or flight hardware.²⁰⁻²²

Development of a UAV platform takes several stages. First the airframe must be developed, which may involve design creation and construction, in the case with a custom design, or just construction, in the case of an already designed and pre-constructed commercial-off-the-shelf airframe (often a model aircraft kit). Next, instrumentation will follow a similar development route, depending on whether it is custom or commercial-off-the-shelf. Then comes ground testing, which may involve loads testing, moment of inertia measurement, and pre-flight combined systems testing. In summation, these stages become extremely costly in terms of resources as well as time. A research group may spend many months or possibly years to develop an aircraft, which may only be flight tested for a limited time.

This paper presents a data set for subscale general aviation aircraft, a 26%-scale Cub Crafters CC11-100 Sport Cub S2 that can be seen in Figure 3, and will be the first of a series of aircraft data sets that will be published online and freely available as part of the Unmanned Aerial Vehicle Database (UAVDB)^a. The database will join several others in providing free access to aeronautical research including the NASA STI Program,²³ the UIUC LSATS and Propeller Datasite,^{24,25} among others.²⁶ The Unmanned Aerial Vehicle Database will be expanded to include many aircraft as they are tested - for example, testing is planned for the Great Planes Avistar Elite (used extensively in previous testing) and a 22% scale Cessna 182 Skylane (currently in development) - as well as data from ground testing such as moment of inertia testing and data reduction techniques that can be used. The database and this paper also include additional details regarding the airframe, instrumentation, flight test plan, as well as related work.



Figure 1. The 26%-scale Cub Crafters CC11-100 Sport Cub S2.

^aThe Unmanned Aerial Vehicle Database is published online at www.uavdb.org

II. Aircraft Description

A. Airframe

The 26%-scale Cub Crafters CC11-100 Sport Cub S2 was developed from a commercially available airframe made by the now defunct model aircraft company, AeroWorks. This airframe has a very good scale representation of the full scale aircraft including relative platform areas and airfoils. 3-view and isometric photos of the aircraft are published on the UAVDB, allowing patrons to trace aircraft geometry. The wing airfoil, the USA-35B, has extensive wind tunnel testing results available as it was very popular in mid 20th century - see NACA Reports 233, 331, 412, and 628.²³

The aircraft was constructed mainly following manufacturer recommendation with the exception of the propulsion system change and the power distribution added. The aircraft was originally designed intended to use an internal combustion gasoline engine, however, the aircraft was adapted to use an electric propulsion system as it provides near constant performance, increased reliability, and low vibrations. A power distribution system was installed onto the aircraft to increase control power redundancy, as it features a dual power regulator, and to help decrease the wiring complexity in the aircraft, as the unit duplicates signals allowing for the instrumentation to read these signals without requiring additional wiring harnesses. Aircraft construction photos can be found in Figure 2. Additionally, photos of aircraft from aircraft Specifications can be found in Tables 1 and 2.

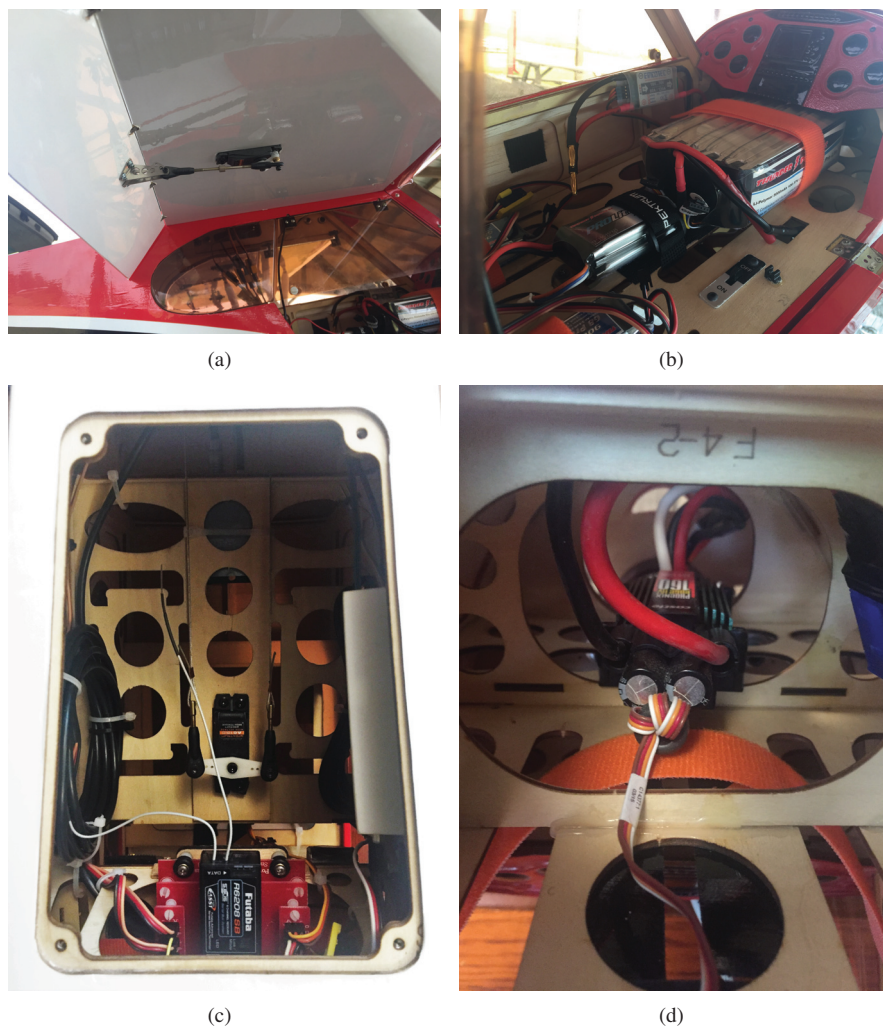


Figure 2. Aircraft construction details: (a) inner wing with flap servo, (b) top tray holding the motor, avionics, and (2) flight control batteries with the motor switch in the background, (c) rear-underside trays holding the rudder pull-pull system and servo, power distribution system with the data acquisition system mounted on the right and left, and (d) underside of the top tray holding the motor electronic speed controller (ESC).

B. Instrumentation

The aircraft was instrumented with an AI Volo DAQ²⁷ data acquisition system. The system operates at 400 Hz and integrates with a 9 degree-of-freedom (9-DOF) XSens MTi-G-700²⁸ IMU with a GPS receiver. A pitot-static probe will be installed half-way down the span of the left wing in the near future. The pilot commands are also recorded by measuring the pulse width modulation (PWM) signals generated by receiver. The propulsion system information is logged by FDAQ through an interfaces with the Castle Creations ESC. Using the sensors, the system is able to log and transmit: 3D linear and angular accelerations, velocities, and position along with GPS location; pitot-static probe airspeed; 3D magnetic field strength and heading; control surface deflections; and motor voltage, current, RPM, and power. Specifications for the instrumentation can be found in Table 3.

Table 1. Airframe physical specifications.

Geometric Properties	
Overall Length	72.0 in (1829 mm)
Wingspan	110.0 in (2794 mm)
Wing Area	1760 in ² (113.5 dm ²)
Wing Aspect Ratio	6.875
Wing Airfoil	USA-35B
Inertial Properties	
Gross Weight	24.2 lb (10.975 kg)
Wing Loading	31.67 oz/ft ² (96.7 gr/dm ²)

Table 2. Airframe component specifications.

Airframe	
Model	AeroWorks 50cc Sport Cub S2
Construction	Built-up balsa and plywood structure, aluminum landing gear, fiberglass cowl, and styrene canopy.
Flight Controls	
Control Surfaces	(2) Ailerons, (2) elevator, rudder, (2) flap, and throttle
Transmitter	Futaba T14MZ
Receiver	Futaba R6008HS
Servos	(7) Spektrum A6150
Power Distribution	SmartFly PowerSystem Sport Plus
Receiver Battery	(2) Thunder Power ProLite RX 25c 2S 7.4V 900 mAh
Propulsion	
Motor	E-Flite Power 360 Outrunner
ESC	Castle Creations Phoenix Edge HV 160
Propeller	Zinger 22x12 Wood
Motor Flight Pack	Thunder Power ProLite 25c 10S 5000 mAh
Motor Power Switch	Emcotec SPS 70V 60/120A

Table 3. Instrumentation specifications.

Data acquisition system	AI Volo FDAQ 400 Hz system
Sensors	
Inertial measurement unit	XSens MTi-G-700 AHRS with GPS
Airspeed sensor	AI Volo Pitot Static Airspeed Sensor
Motor sensor	AI Volo Castle ESC Interface
Power	
Regulator	Built into DAQ
Battery	Thunder Power ProLiteX 3S 1350 mAh

III. Test Plan

A comprehensive test plan was developed that encompassed a variety of maneuvers with many permutations. The planned maneuvers would allow the end user to build and/or verify various aerodynamic, performance, and handling models for the aircraft. These maneuvers were conducted by a pilot who flew the aircraft and flight coordinator who relayed the flight commands and monitored the battery state for the duration of the flight test.

Table 4. Flight Test Maneuvers Tested

Maneuver	Flap Configuration	Description	Purpose / Characterize
Idle Descent	Clean Half-Flaps	Descent using idle power with different amounts of trim with limited elevator deflection	Drag and neutral point
Phugoid	Clean Full-Flaps	Entry with aircraft trimmed and elevator deflected to change airspeed	Dynamic longitudinal stability
Pitch Response	Clean	Elevator momentarily deflected with minimum pitch rate	Longitudinal dynamics in response to elevator
Roll Response	Clean	Ailerons momentarily deflected with minimum roll rate	Lateral dynamics in response to aileron
Yaw Response	Clean	Rudder momentarily deflected Rudder deflected and held	Lateral dynamics in response to rudder Lateral to longitudinal control coupling
Power-Off Stall	Clean Half-Flaps Full-Flaps	Entry with wings level; limited elevator deflection full elevator deflection limited elevator deflection full elevator deflection limited elevator deflection full elevator deflection	Aerodynamics and dynamical behavior for high angle of attacks
Power-Off Spin	Clean Half-Flaps Full-Flaps	Entry with wings level; limited elevator deflection full elevator deflection limited elevator deflection full elevator deflection limited elevator deflection full elevator deflection	Entry and recovery and dynamic behavior of aircraft during spin



Figure 3. The 26%-scale Cub Crafters CC11-100 Sport Cub S2 during takeoff.

IV. Results

The results presented here are a subset of the complete data set collected and as such provide a sample representation of what is available. All of the maneuvers recorded, among the rest, are available on the UAVDB website, including plots of trajectories and time history of state data, and flight data. Maneuvers were performed following the test plan presented in Table 4. About a dozen flight tests were performed, each of which contained multiple maneuvers that varied in the type (idle descent, phugoid, etc.) and permutation (limited deflection, full deflection, no flap, half flap, full flap, etc.). The data was cut based on written notes of what was performed along with visual inspection of the data using aircraft trajectories and time history of state data. The resulting maneuver data sets were then filtered to remove erroneous measurements of maneuvers, such as those resulting from external environmental effects (wind and turbulence), and to provide the best representation of the aircraft behavior.

The idle decent maneuvers are given on Fig. 4-7, for zero and half flap settings. The flight speed of the aircraft decreases from 20 to 12 m/s as the flap settings changes from the zero to half setting. The trajectories followed by the aircraft depend upon wind direction, the initial heading, and flight speed of the aircraft when the maneuver was conducted. Though the trajectories differ slightly, the response of the aircraft is the same for both flight test cases. The elevator responses are shown in Fig. 8-13, where the aircraft pitch will change as a response to the elevator input. As the aircraft was trimmed and balanced to the manufacturer specifications, it tended to settle back to its trim settings for up elevators due to the positive pitching moment of the wing. When down elevator was applied, the aircraft continued to pitch nose down, as the aircraft would trim at a lower angle of attack. The phugoids maneuvers shown in Fig. 14-17 all settled back to the aircraft trim settings, where the settling time increased as the flap settings increased from zero to full flaps. This behavior is very atypical for aircraft, but is suspected to be related to the STOL nature of the Sport Cub S2. When the aircraft is put into a stall as shown in Fig. 18-23, it returned back into a stable configuration without requiring pilot input. When the aircraft reached its stall angle, it pitched downward as the wing surface stalled before the horizontal surface.

The roll responses shown in Fig. 24-27, showed that the aircraft will roll in response to the aileron input until the pilot counteracts it. If the aircraft does not experience a counteracting aileron as an input, the aircraft will turn and bank until settles. As the aircraft is designed to be laterally stable, small rudder oscillations such as those shown in Fig. 28 and 29 will cause a it to side-slip slightly though it will return to its original heading. When the rudder is held longer, as seen in Fig. 27 and 31, the aircraft will begin to bank as side-slip causes a rolling moment to act on the aircraft. The spin maneuvers in Fig. 32-35 were conducted by applying full rudder and up elevator to causing the aircraft to upset and enter a spin. All of spin maneuvers settled back into stable configuration within half of a revolution once the pilot released the control input.

V. Future Work

The Unmanned Aerial Vehicle Database will be expanded to include additional aircraft as they are tested - including the Great Planes Avistar Elite and a 22% scale Cessna 182 Skylane. Additionally this data base will also include moment of inertia of the aircraft which will be measured through testing.²⁹The flight testing of these aircraft will also be improved upon as it will be conducted using automated testing, which will reduce erroneous recordings and ensure consistent tests.

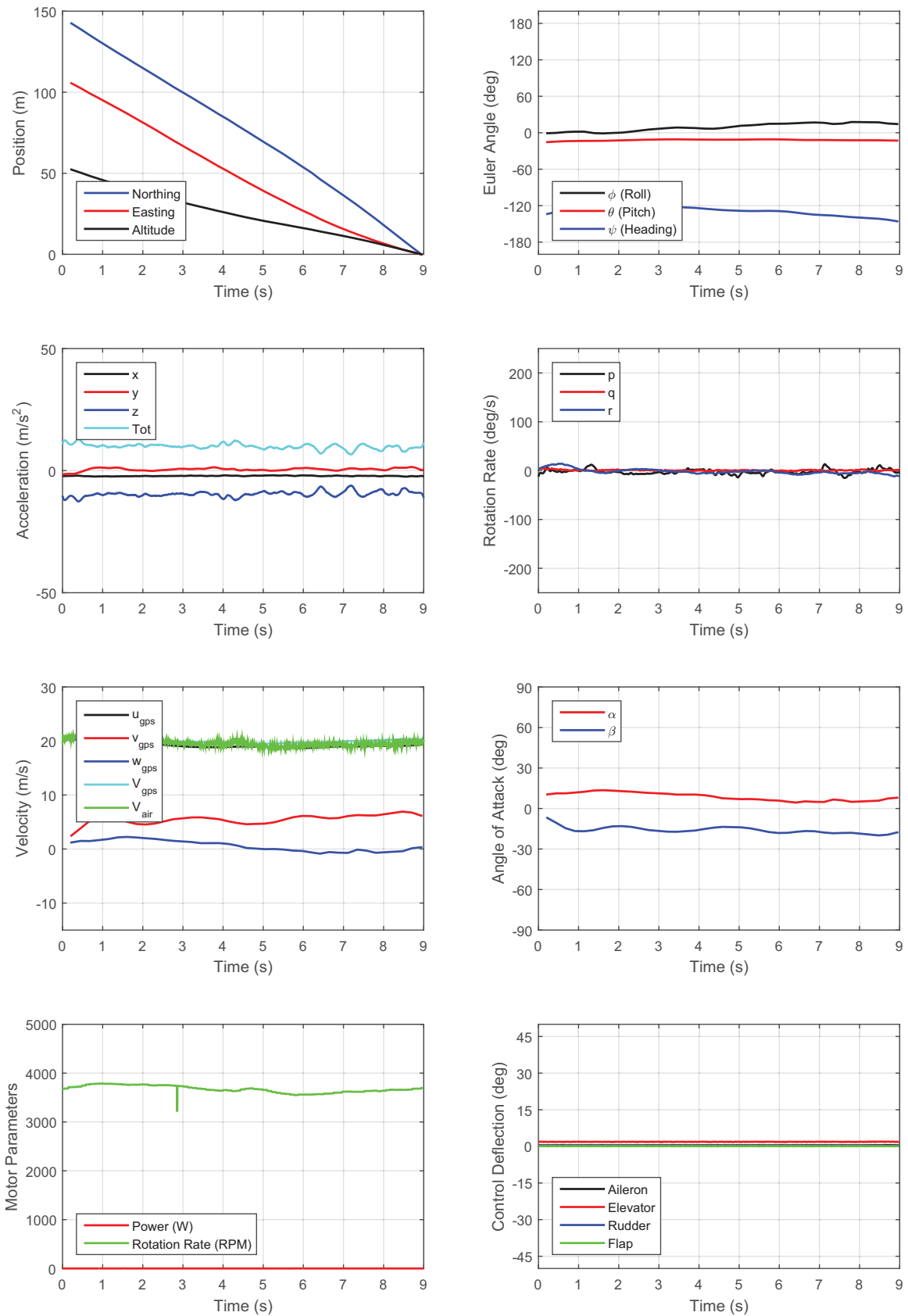


Figure 4. Time history of aircraft state during idle descent with no flaps.

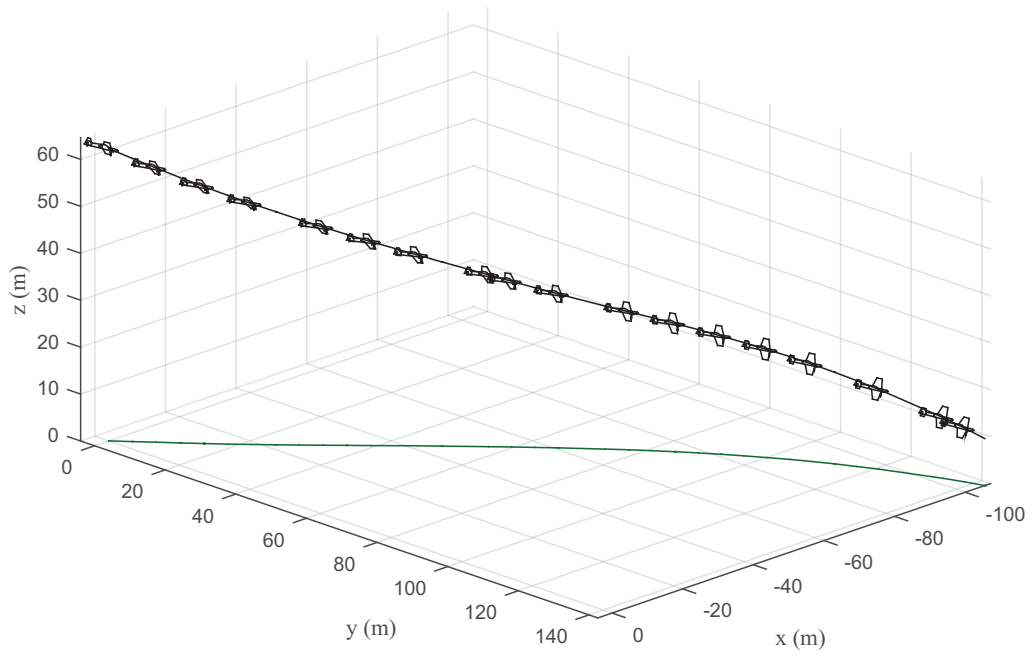


Figure 5. Trajectory of the aircraft during idle decent with no flaps.

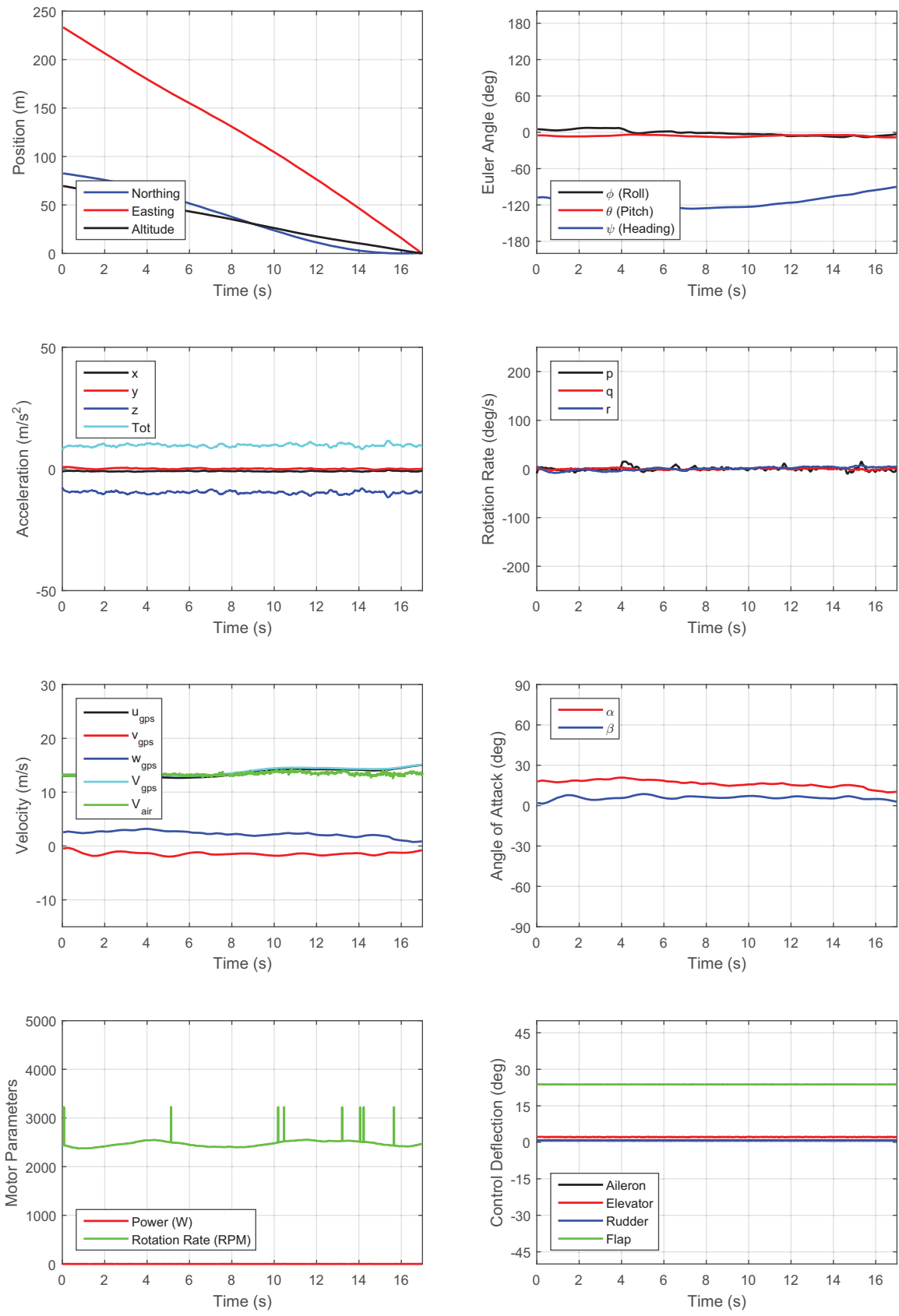


Figure 6. Time history of aircraft state during idle decent with half flaps.

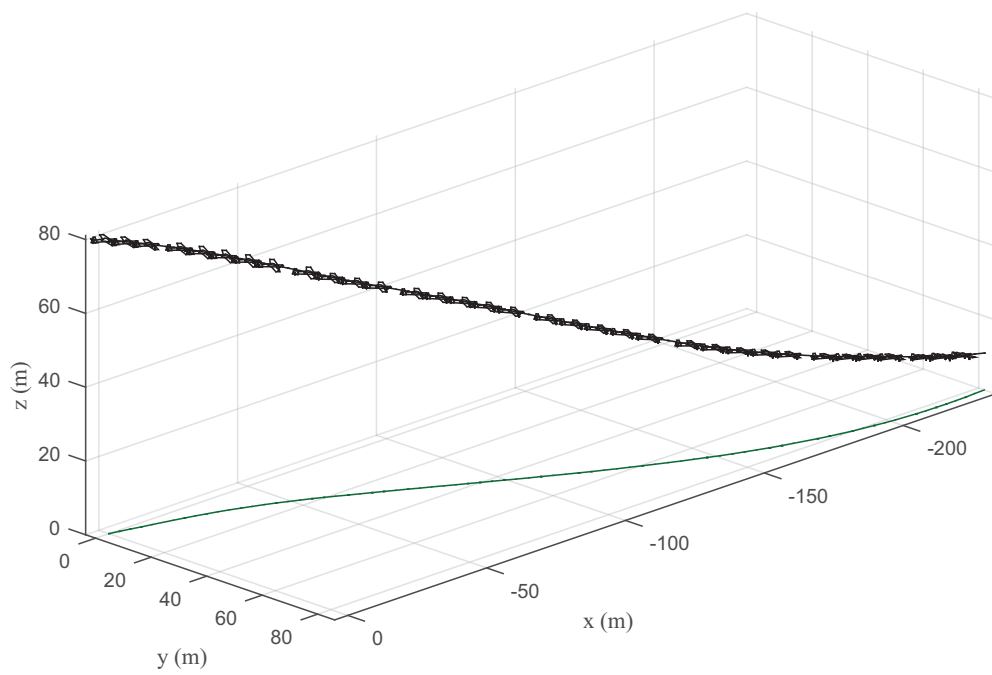


Figure 7. Trajectory of the aircraft during idle decent with half flaps.

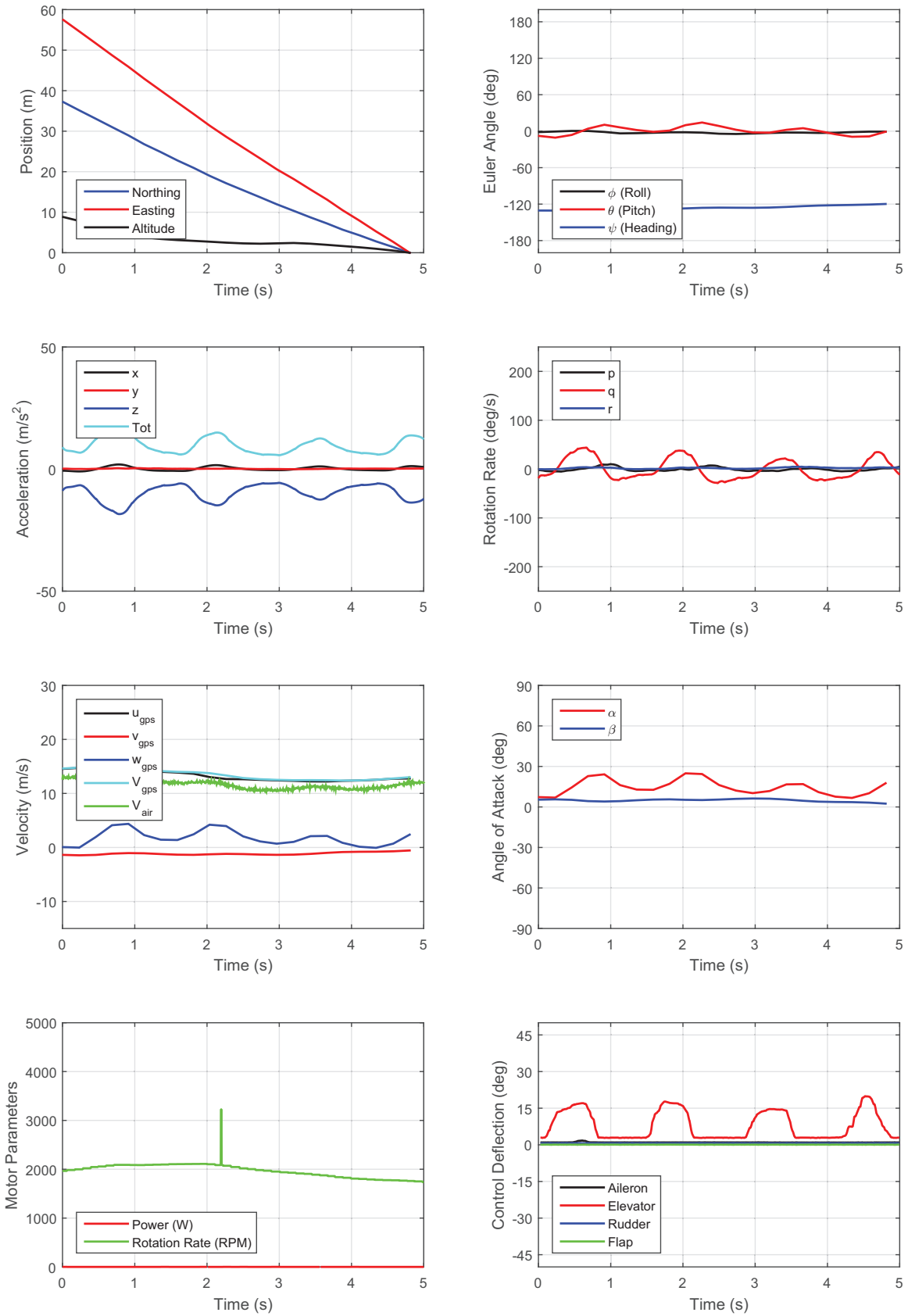


Figure 8. Time history of aircraft state during up elevator response.

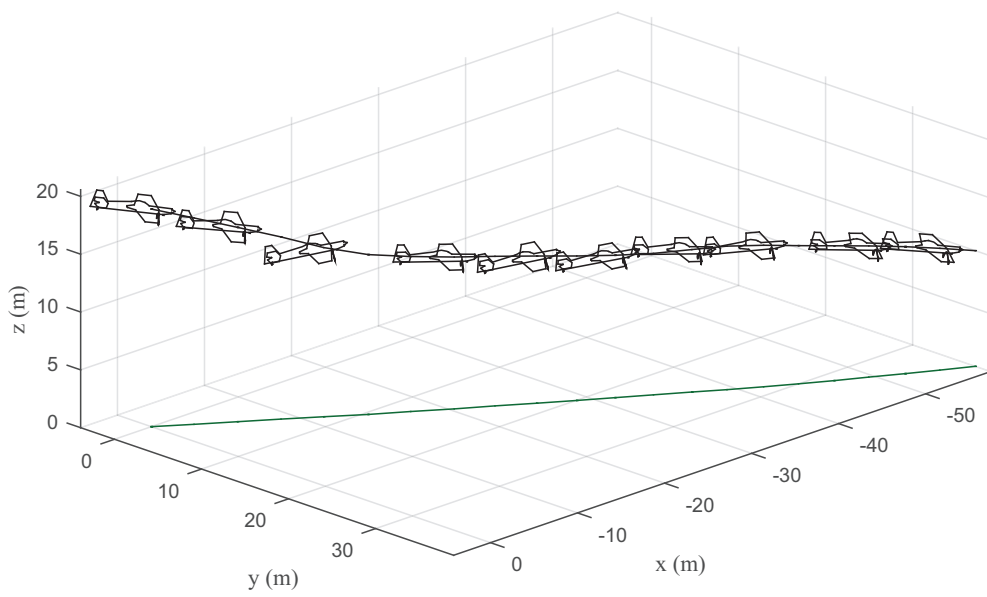


Figure 9. Trajectory of the aircraft during up elevator response.

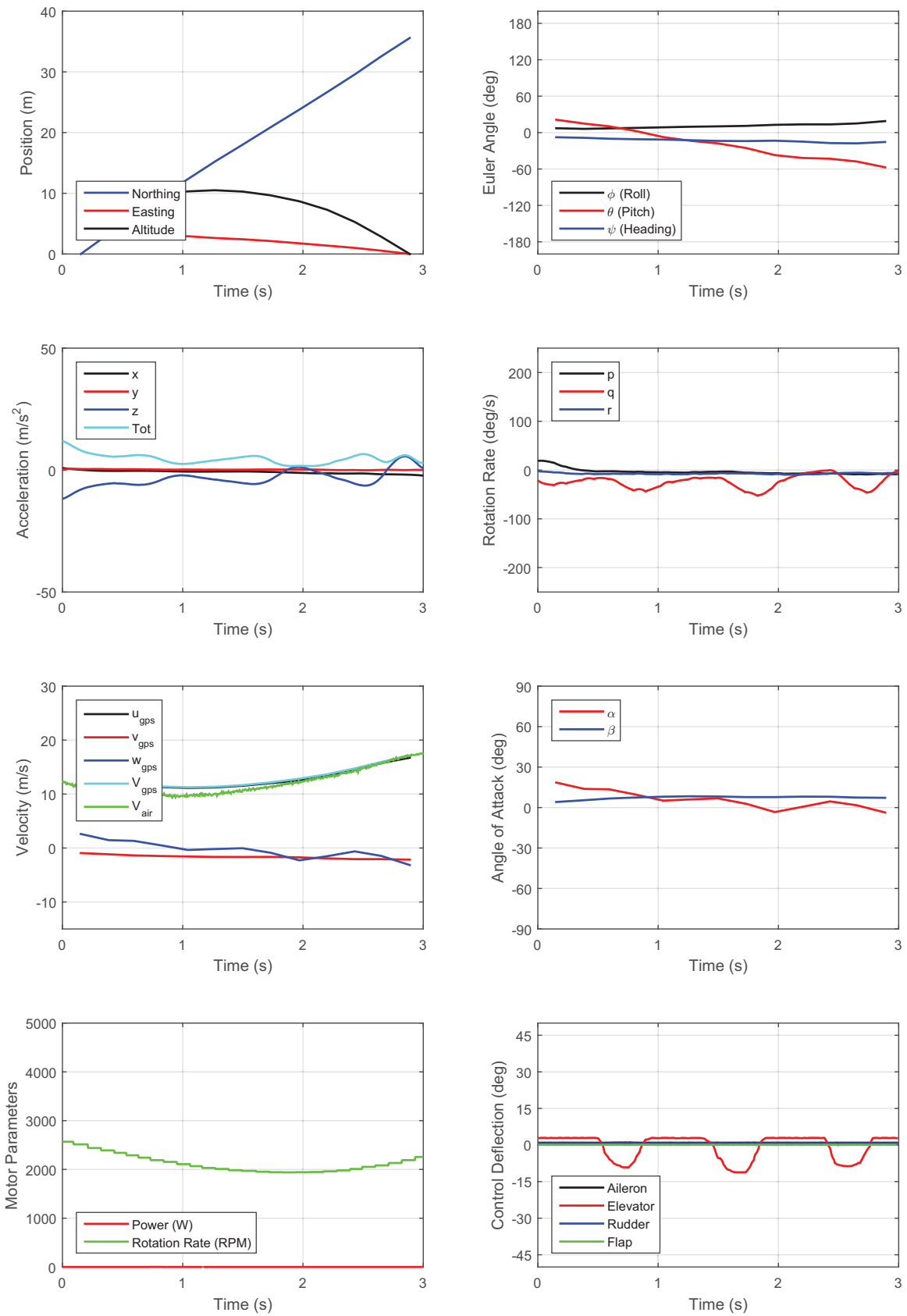


Figure 10. Time history of aircraft state during down elevator response.

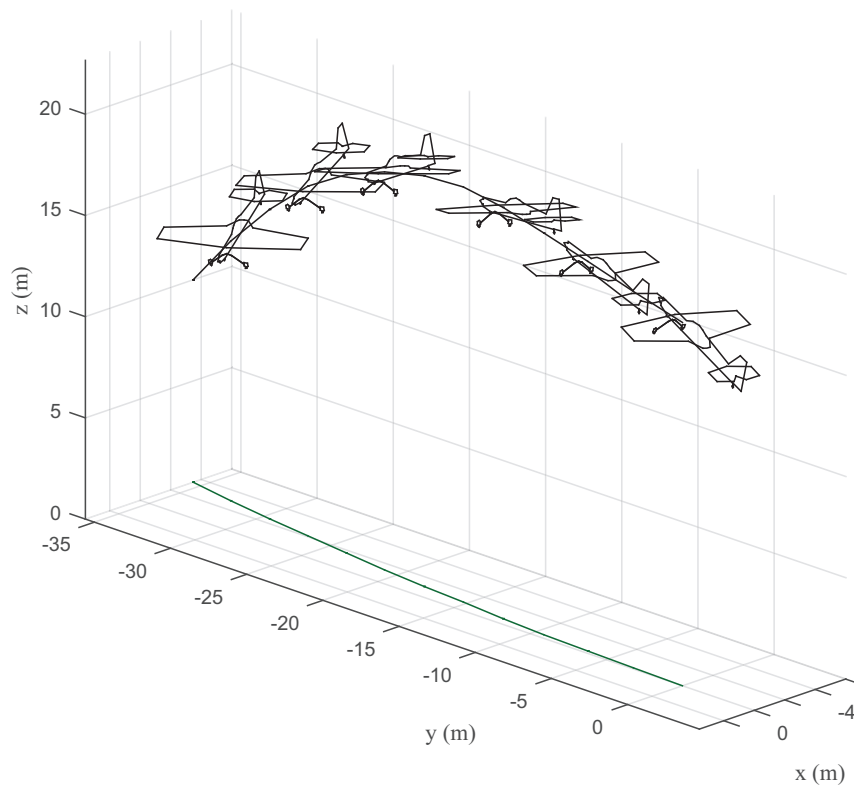


Figure 11. Trajectory of the aircraft during down elevator response.

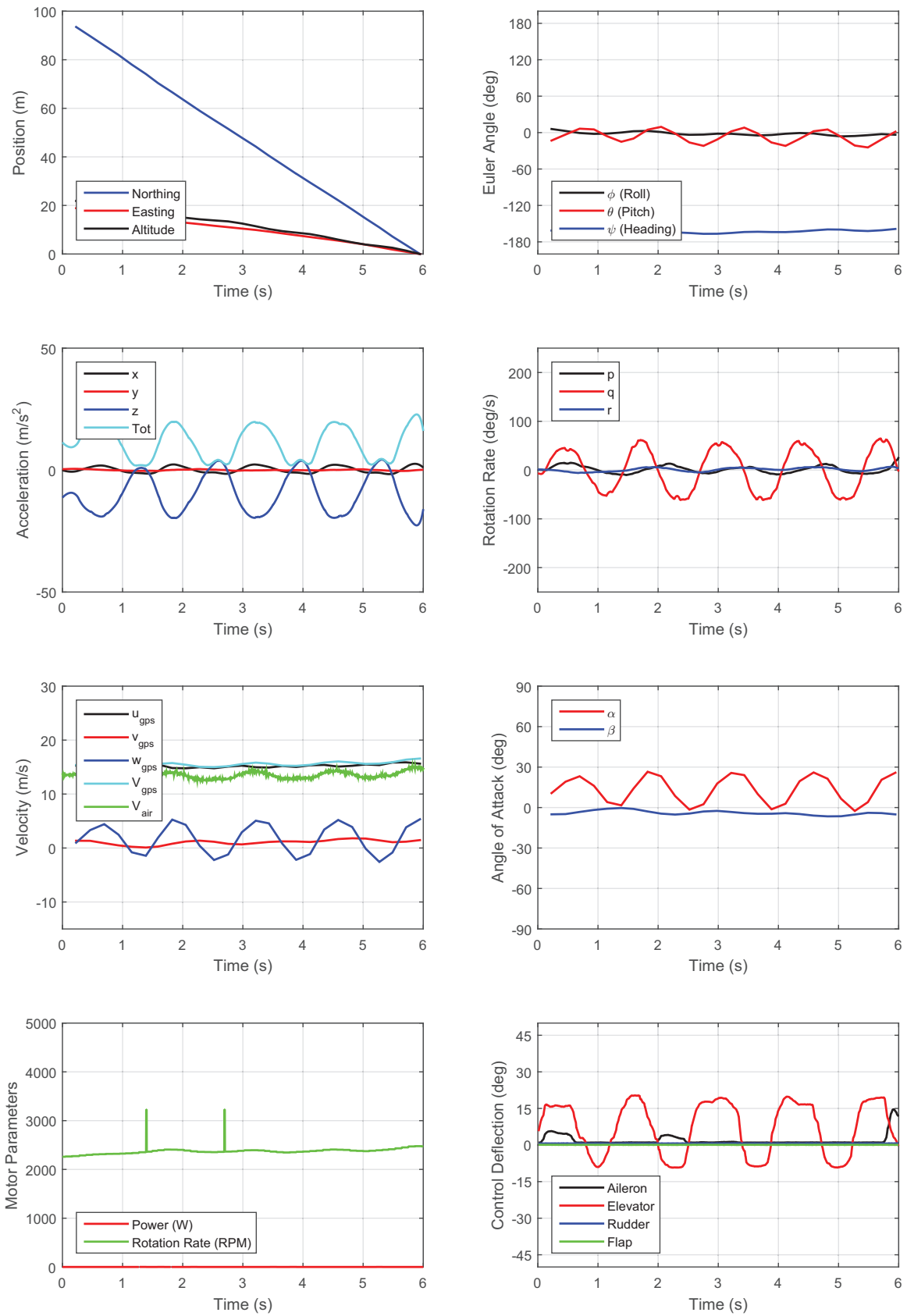


Figure 12. Time history of aircraft state during up and down elevator response.
15 of 39

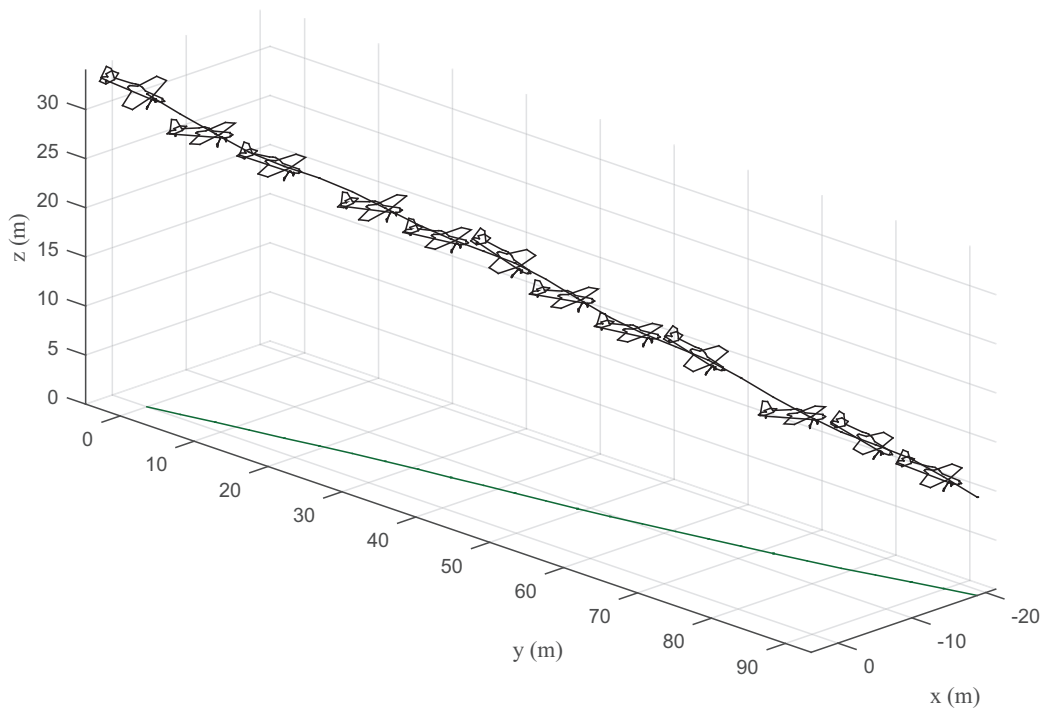


Figure 13. Trajectory of the aircraft during up and down elevator response.

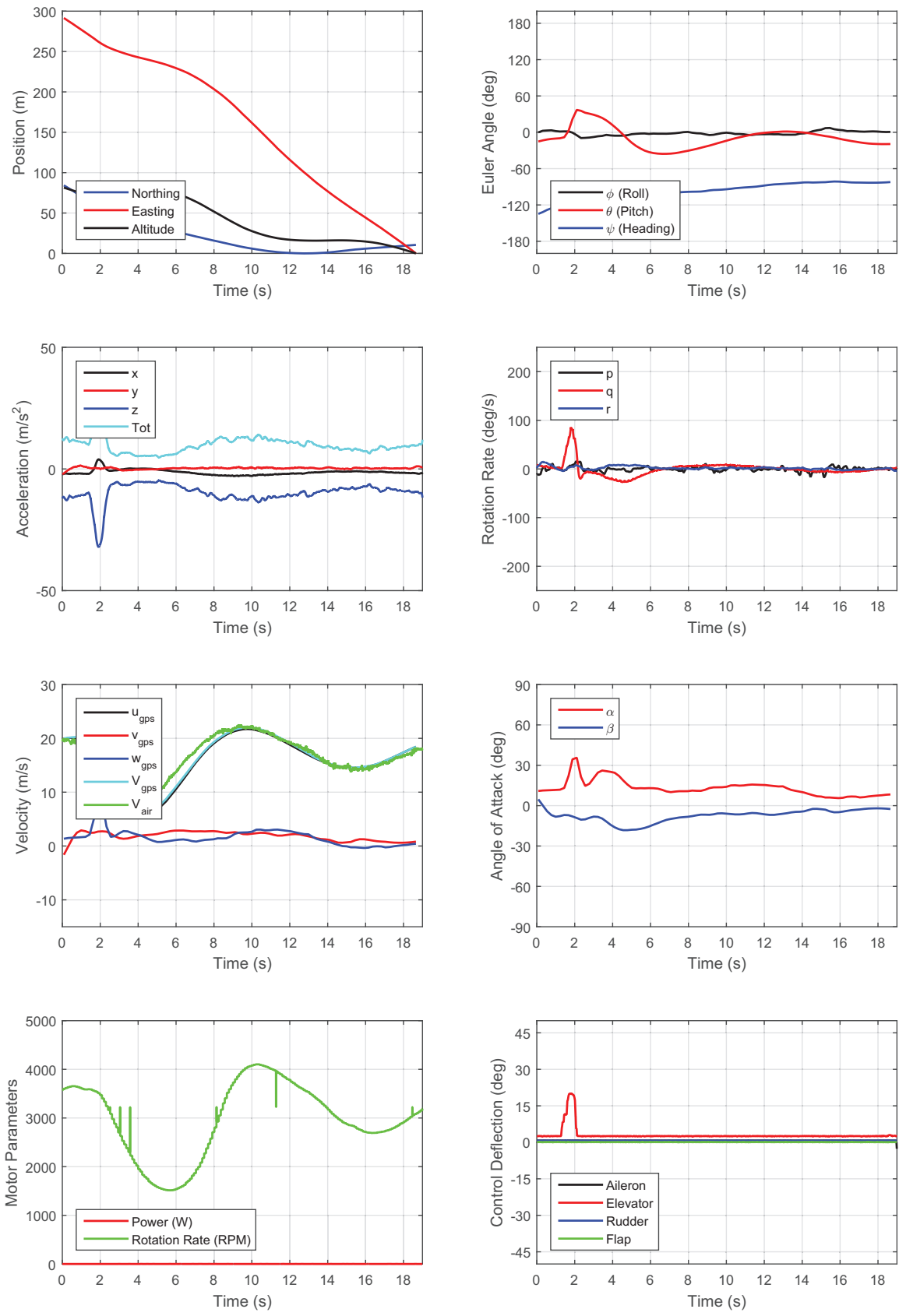


Figure 14. Time history of aircraft state during a phugoid with no flaps.

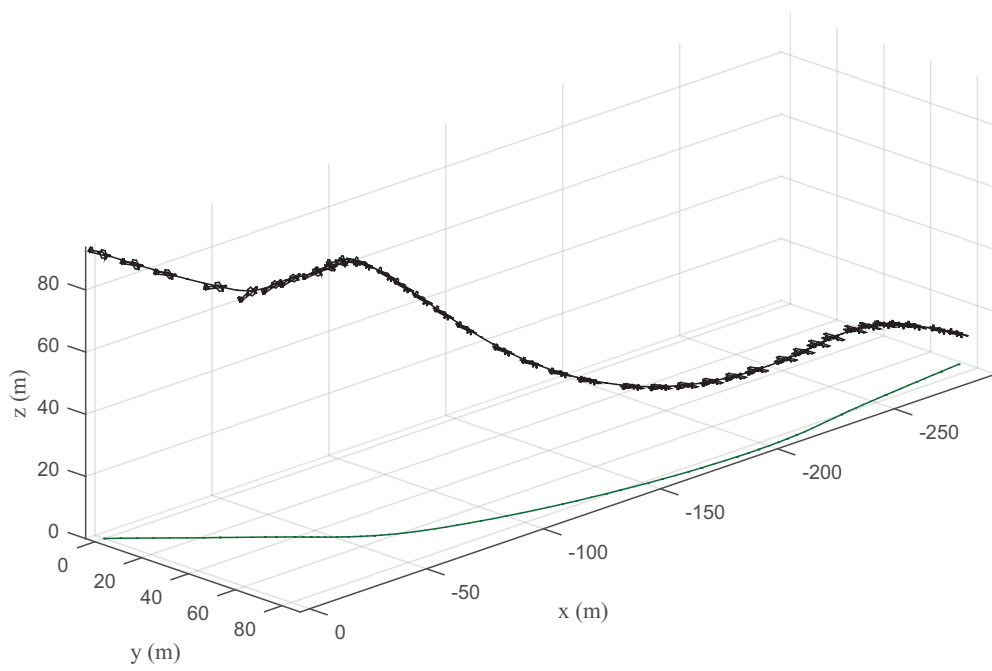


Figure 15. Trajectory of the aircraft during phugoid with no flaps.

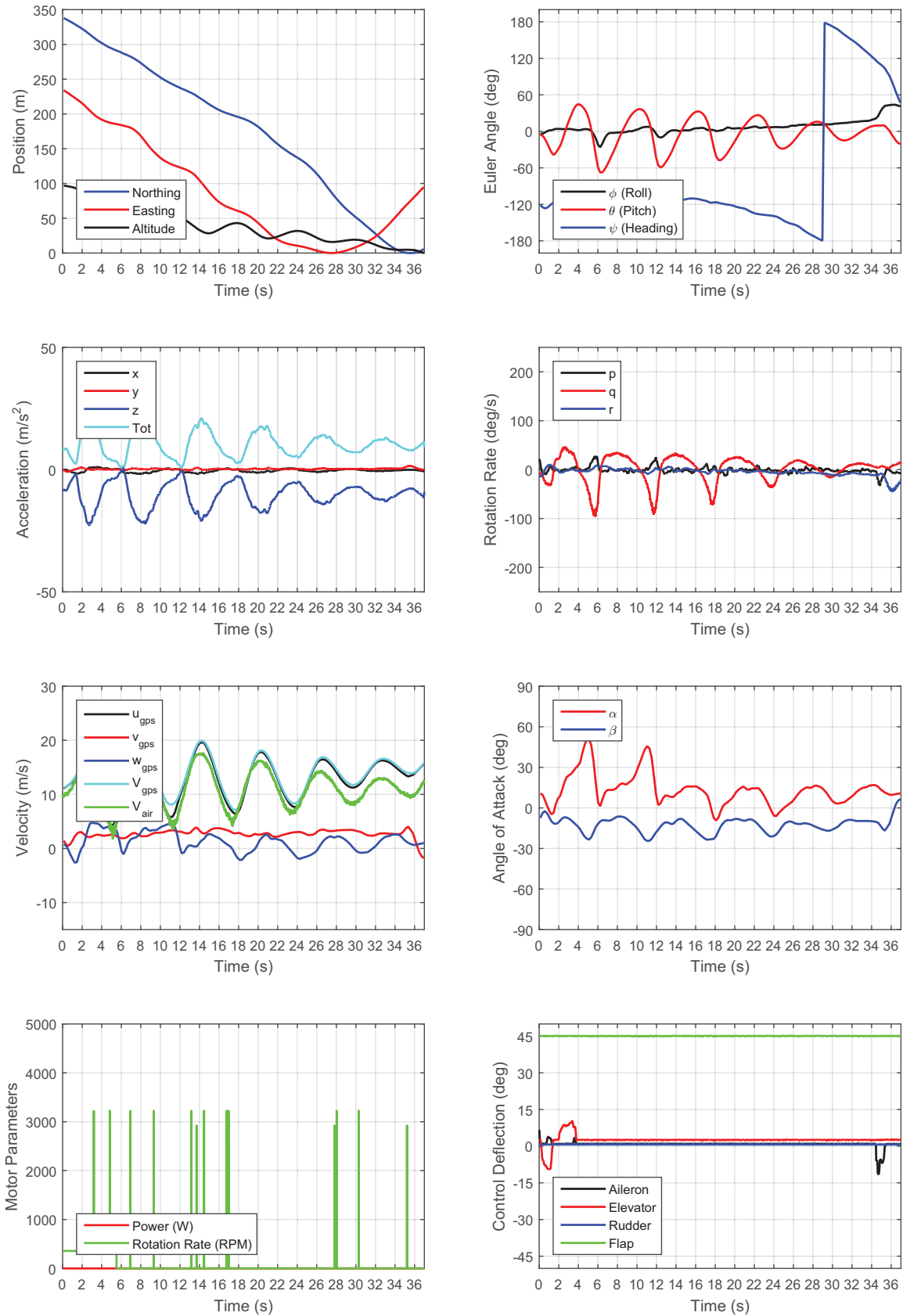


Figure 16. A time history of aircraft state during a phugoid with full flaps.

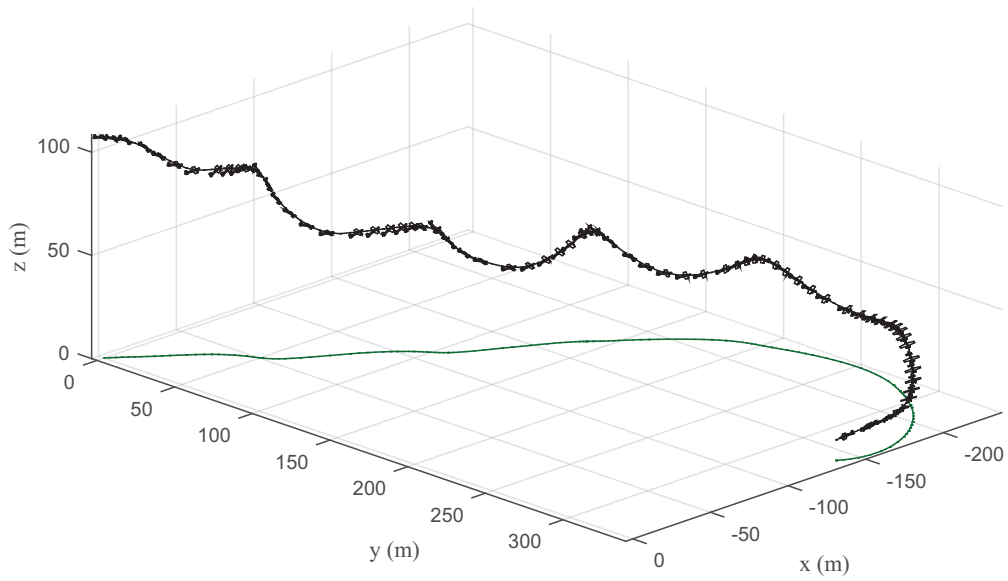


Figure 17. Trajectory of the aircraft during phugoid with full flaps.

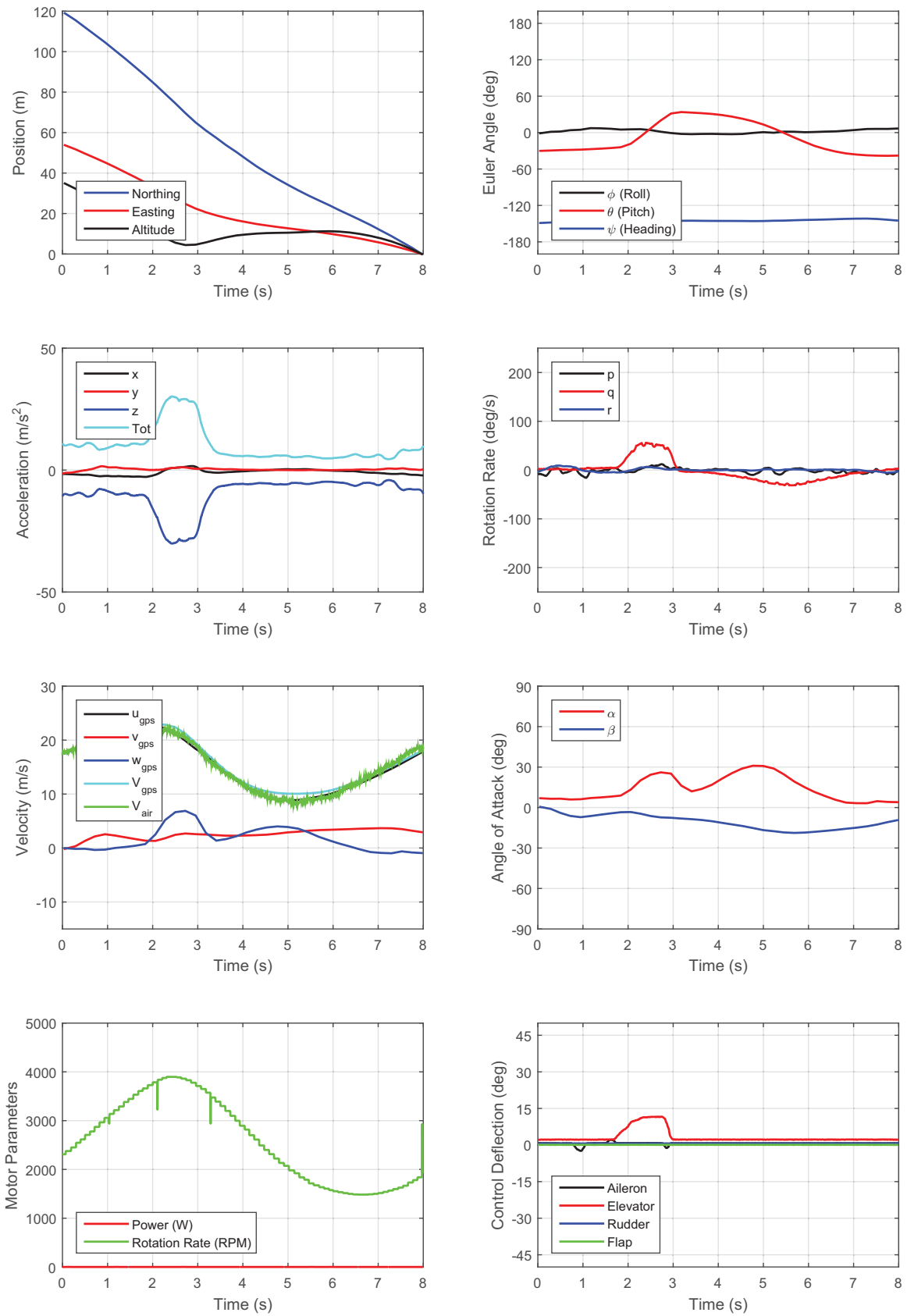


Figure 18. Time history of aircraft state during stall with zero flap.

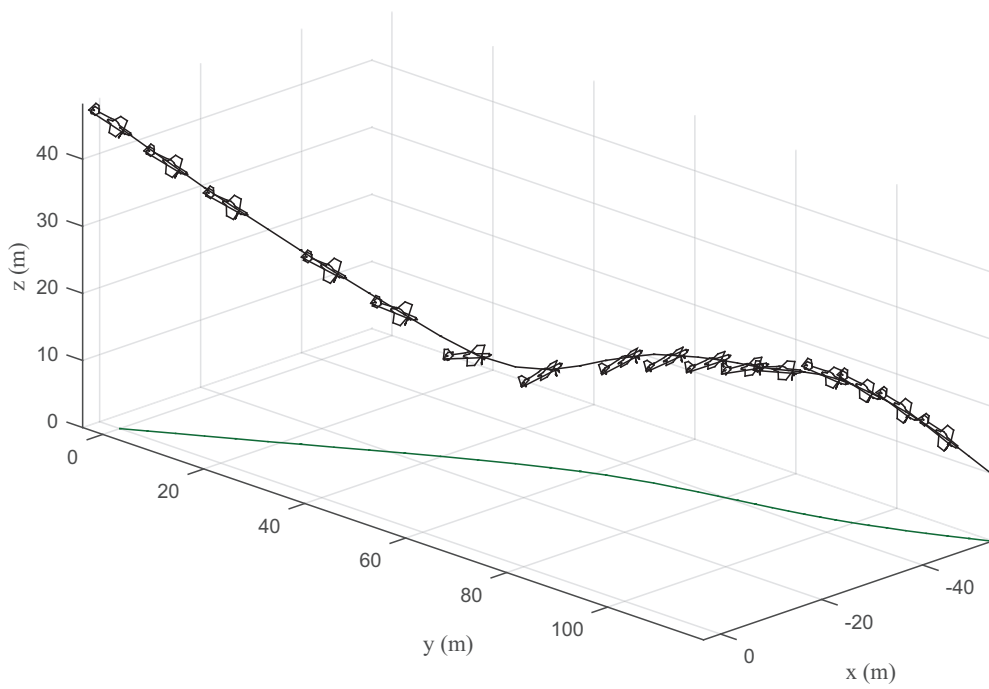


Figure 19. Trajectory of the aircraft during stall with zero flap.

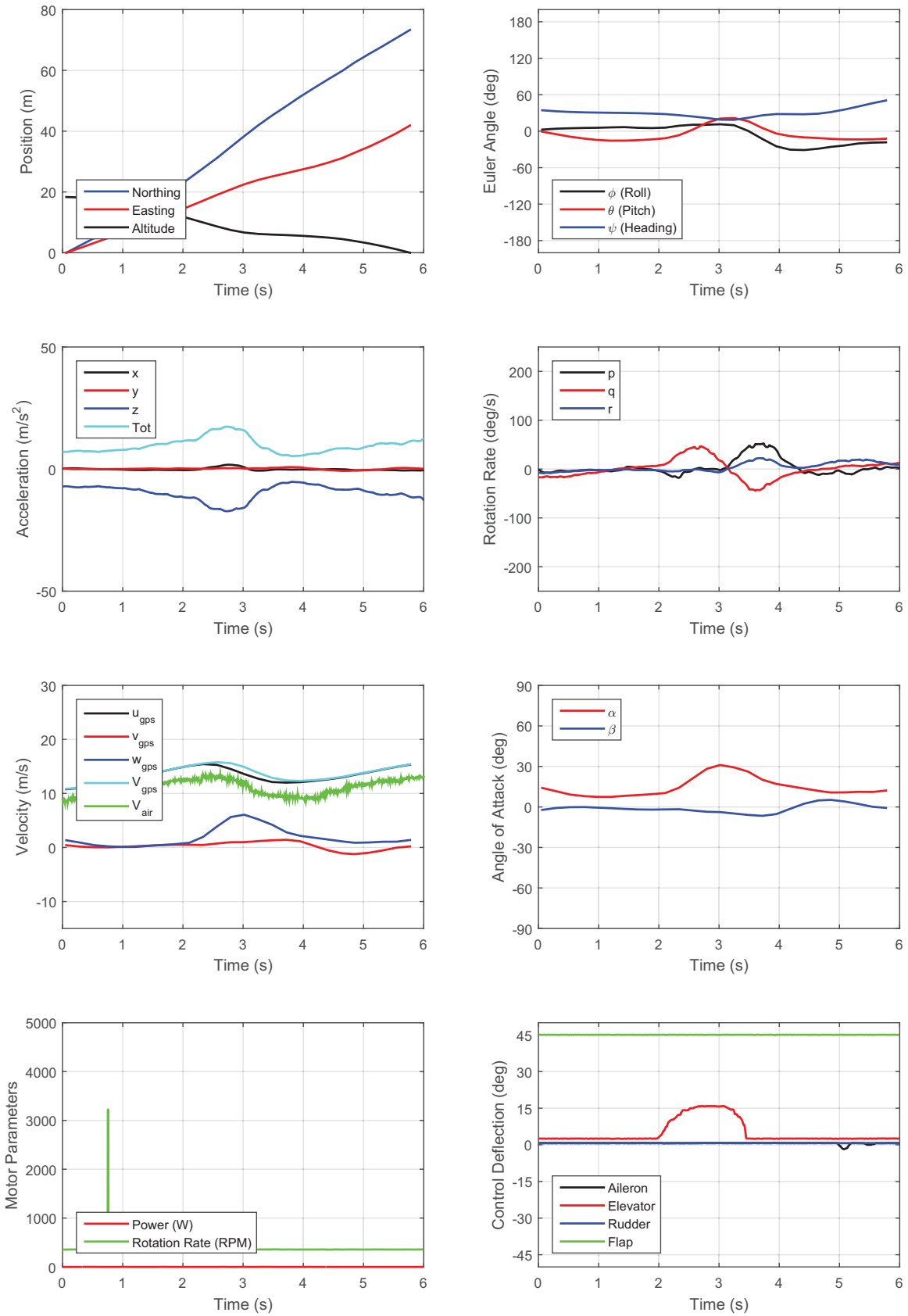


Figure 20. Time history of aircraft state during stall with full flap.

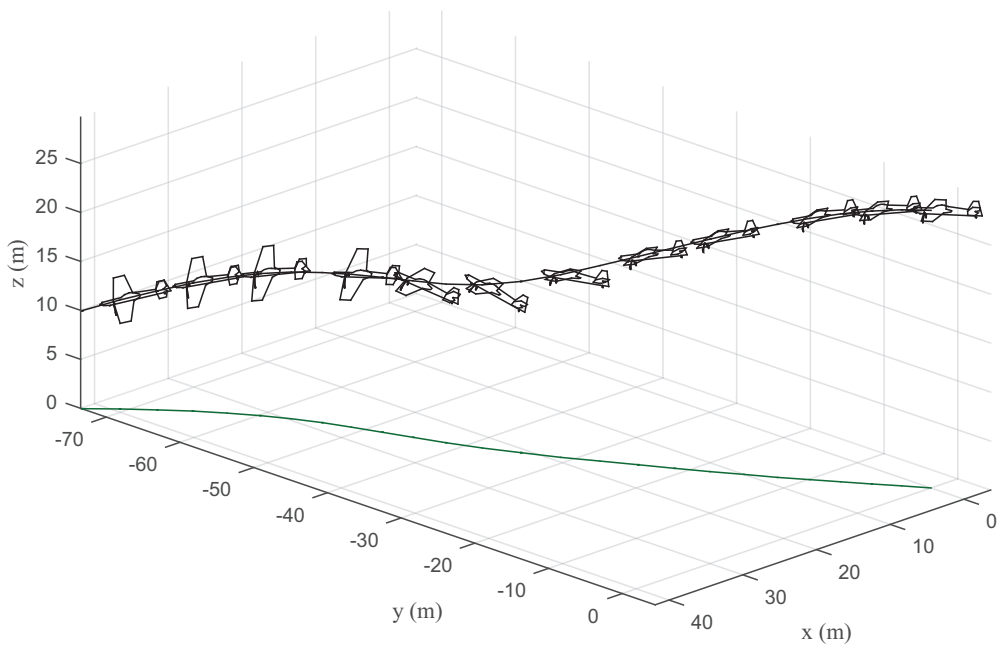


Figure 21. Trajectory of the aircraft during stall with full flap.

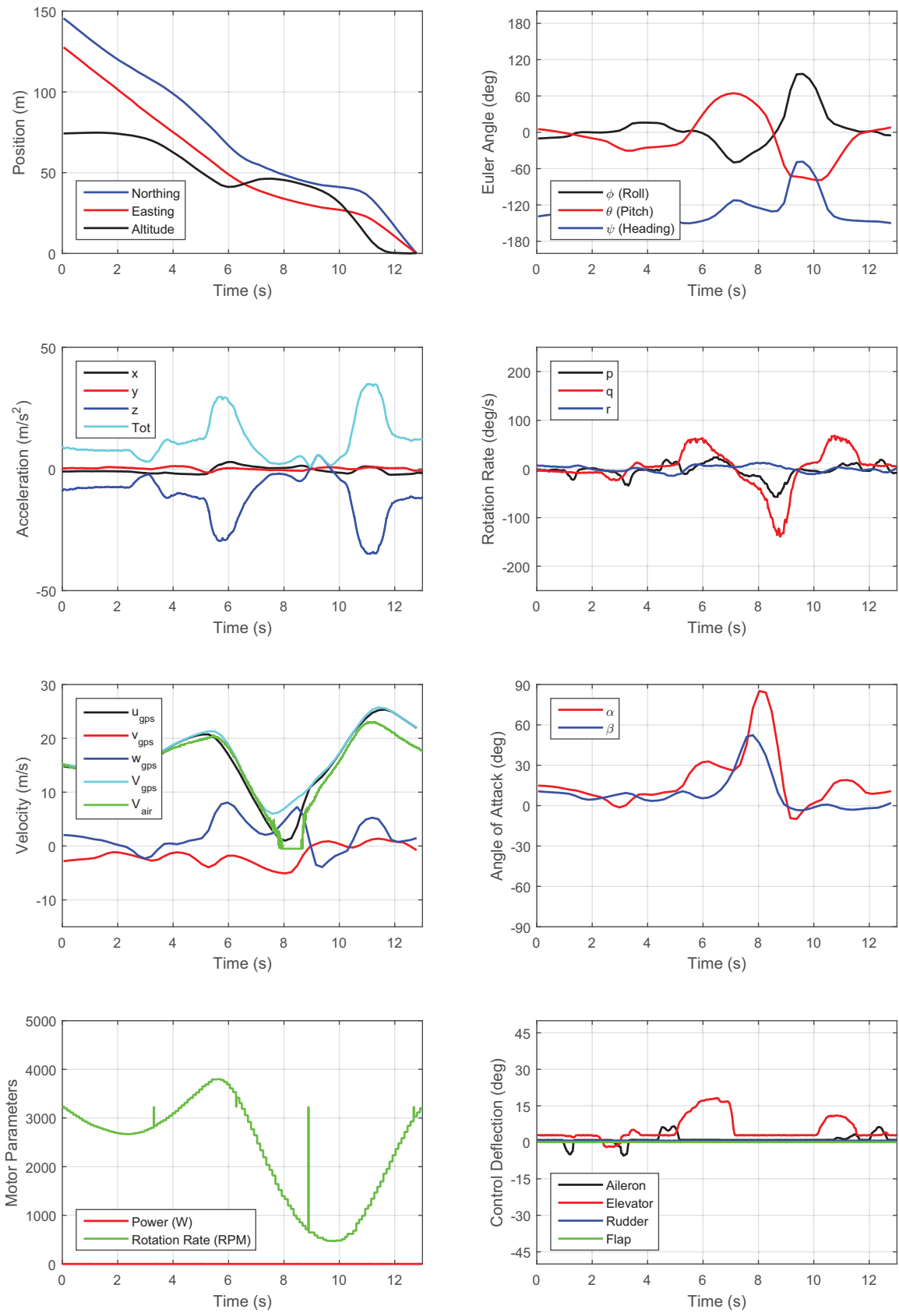


Figure 22. Time history of aircraft state during deep stall with zero flap.

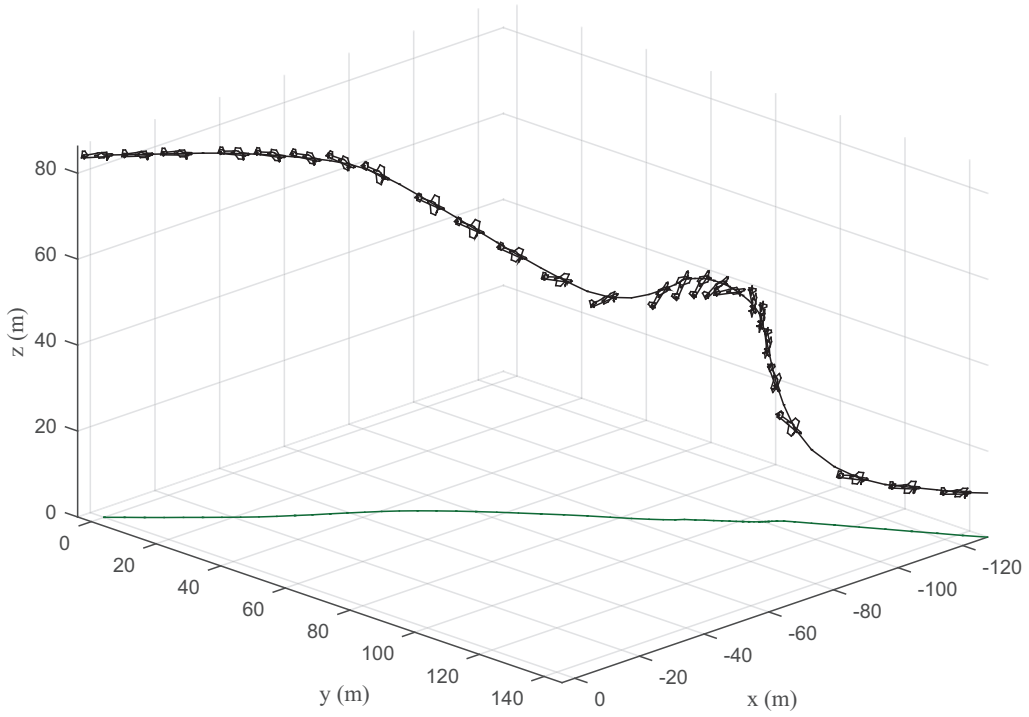


Figure 23. Trajectory of the aircraft during deep stall with zero flap.

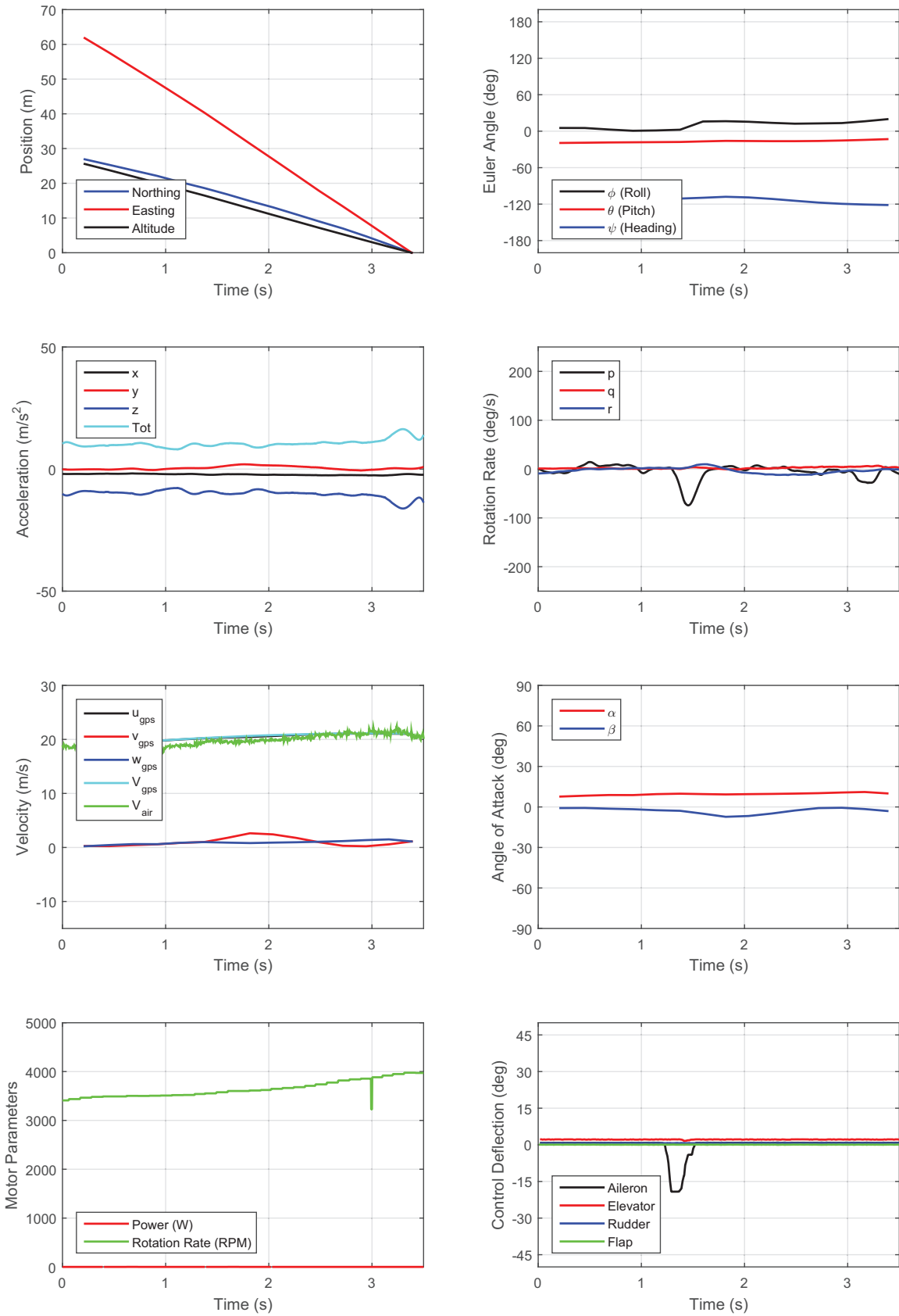


Figure 24. Time history of aircraft state during a roll response with left aileron.

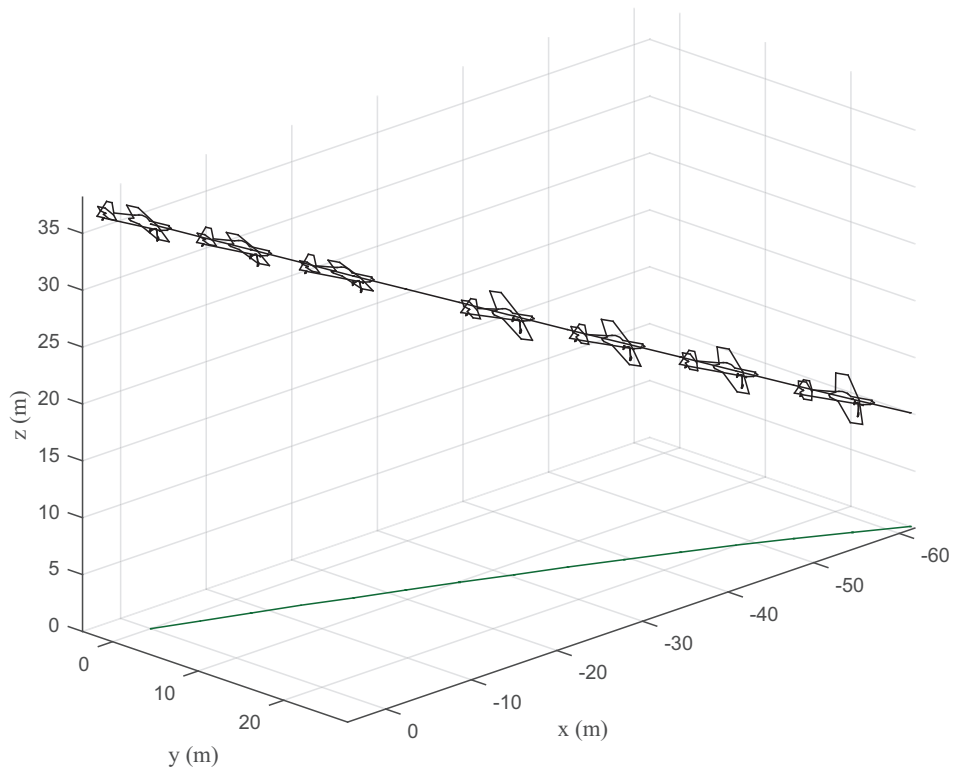


Figure 25. Trajectory of the aircraft during a roll response with left aileron.

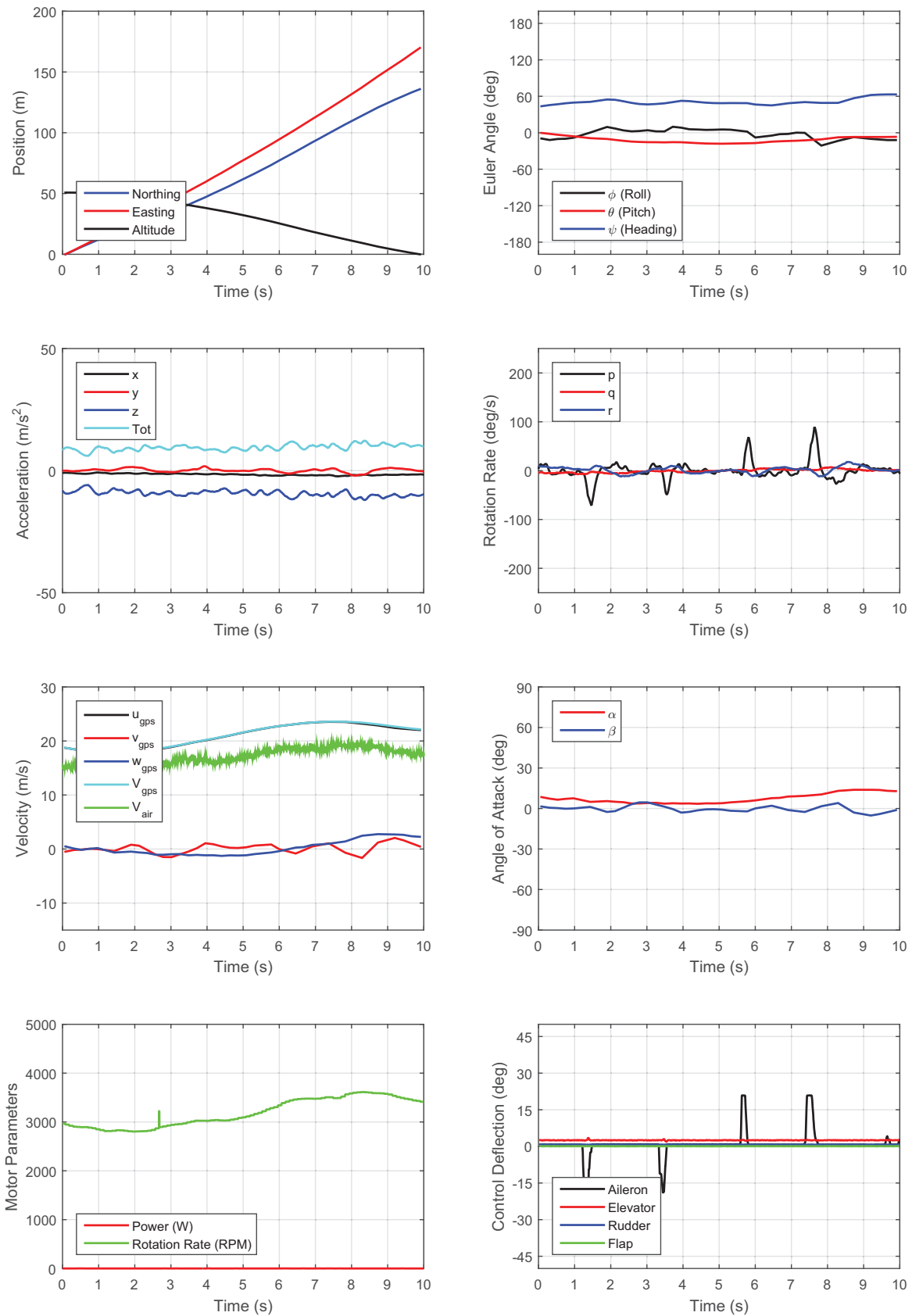


Figure 26. Time history of aircraft state during a roll response with left and right ailerons.

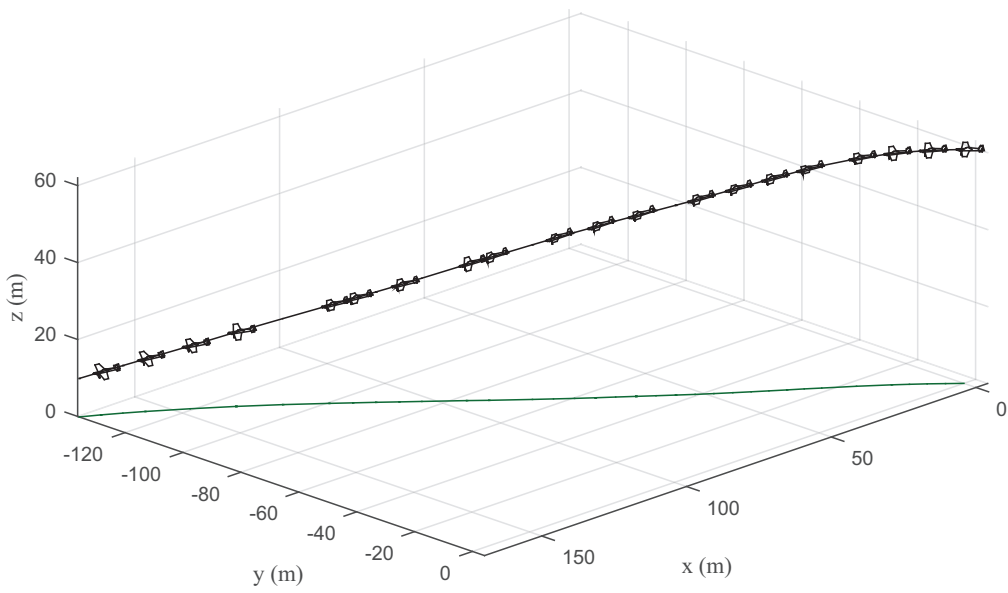


Figure 27. Trajectory of the aircraft during a roll response with left and right ailerons.

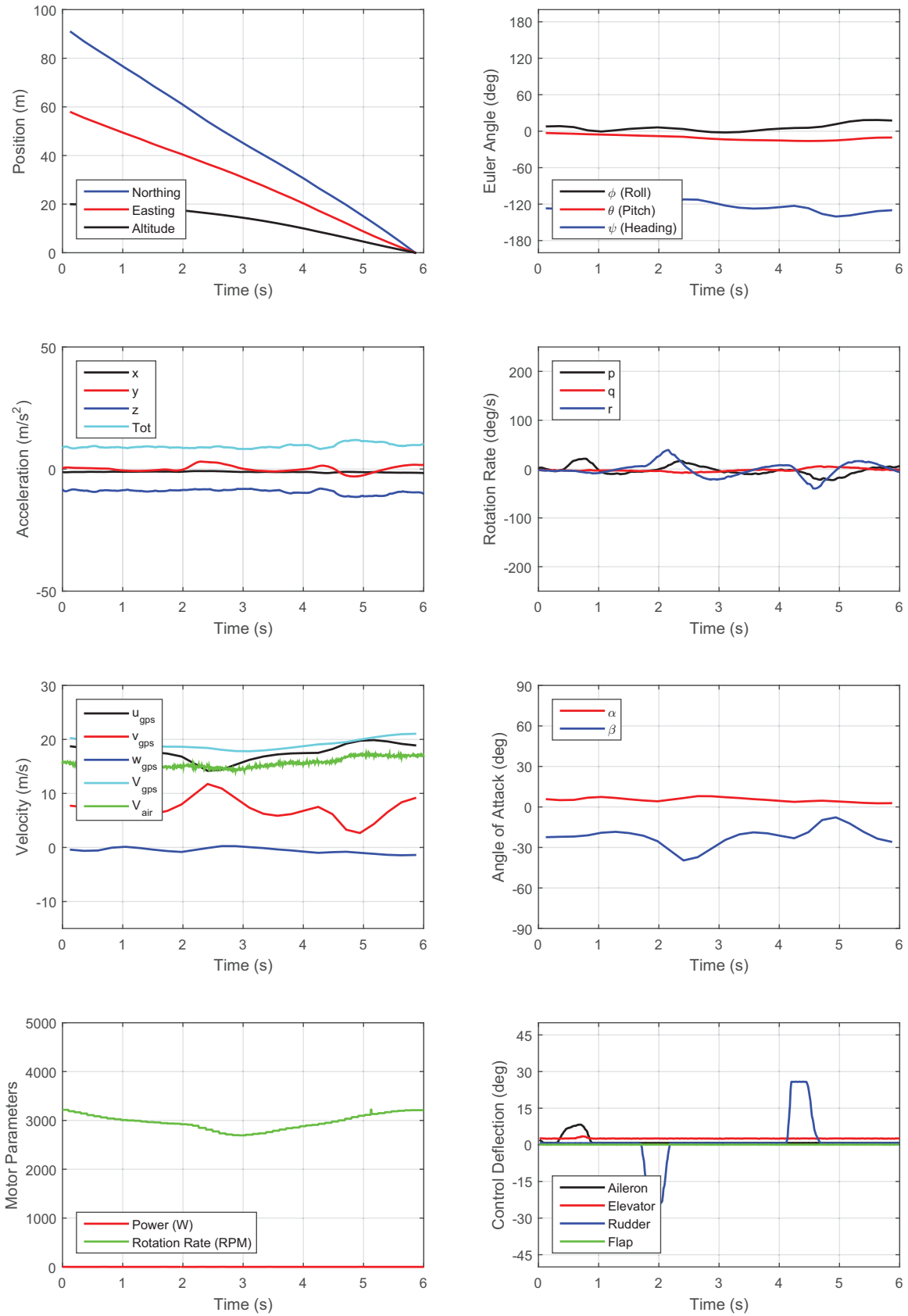


Figure 28. Time history of aircraft state with left and right rudder inputs.

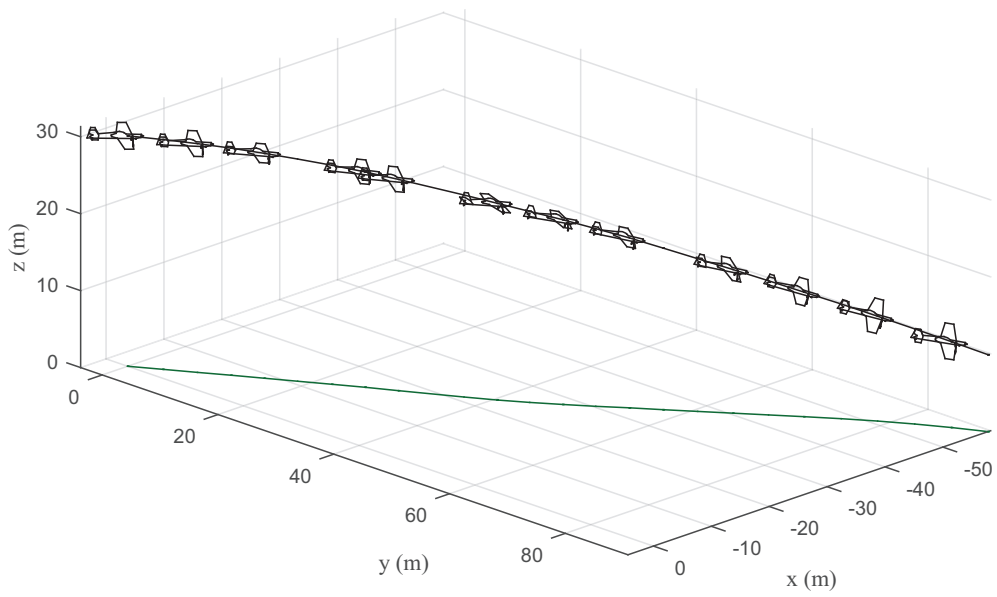


Figure 29. Trajectory of the aircraft with left and right rudder inputs.

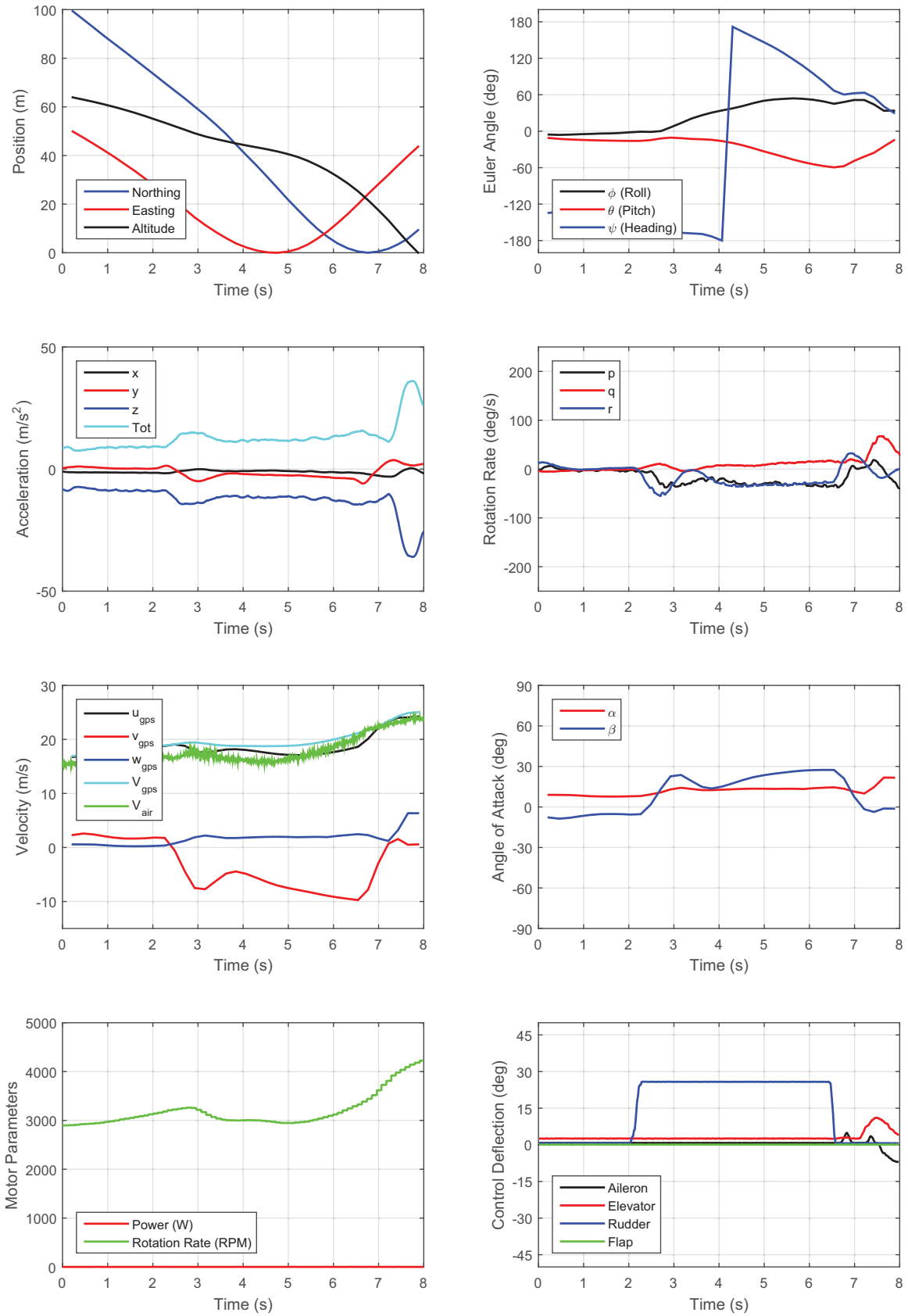


Figure 30. Time history of aircraft state with continuous rudder input.

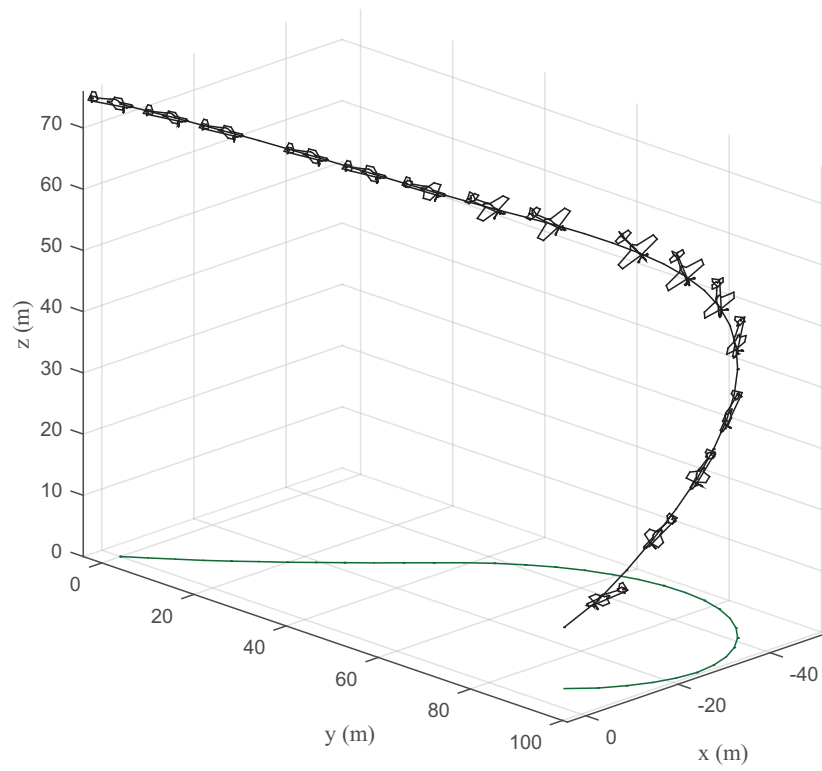


Figure 31. Trajectory of the aircraft with continual rudder input

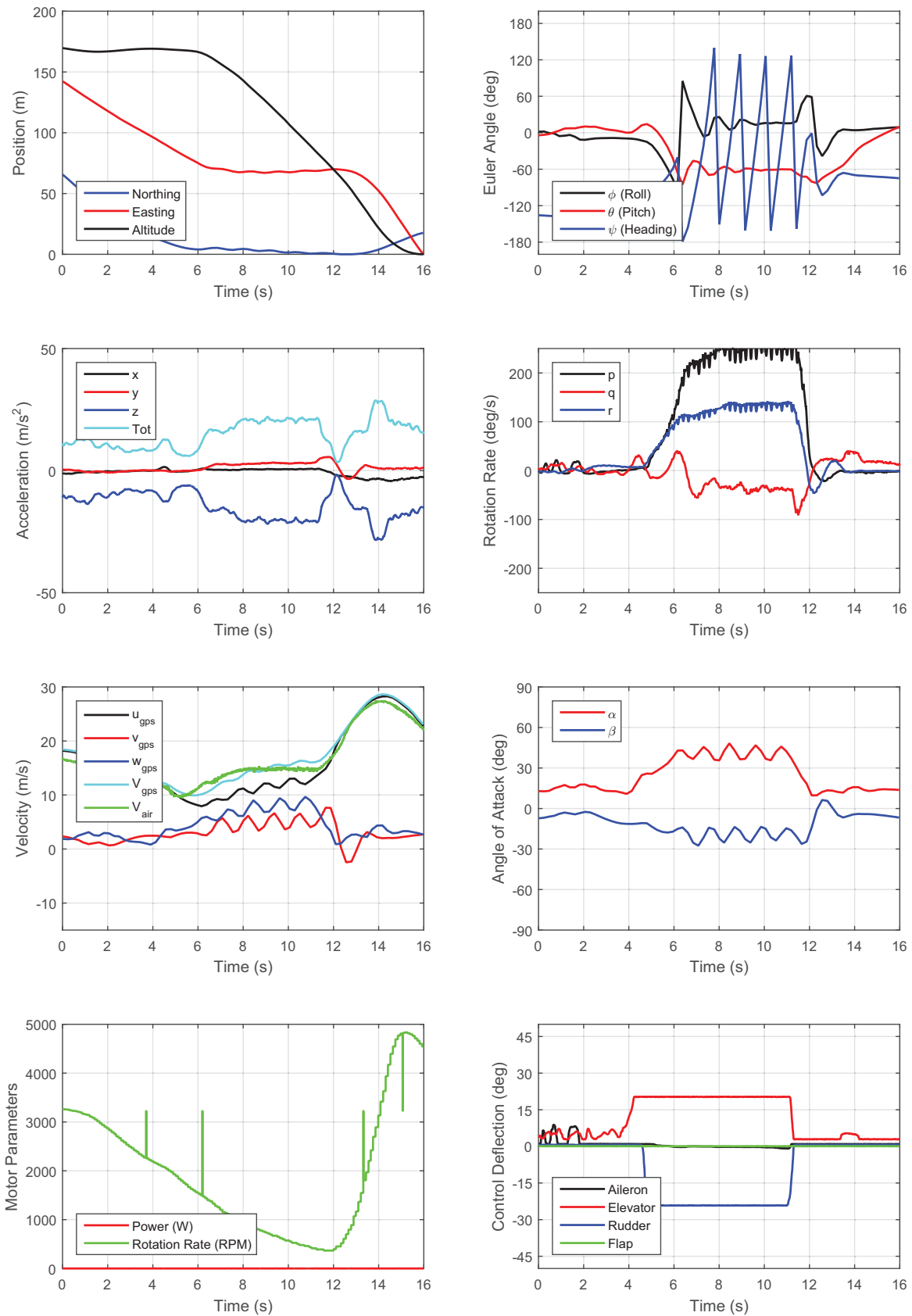


Figure 32. Time history of aircraft state during spin with zero flap.

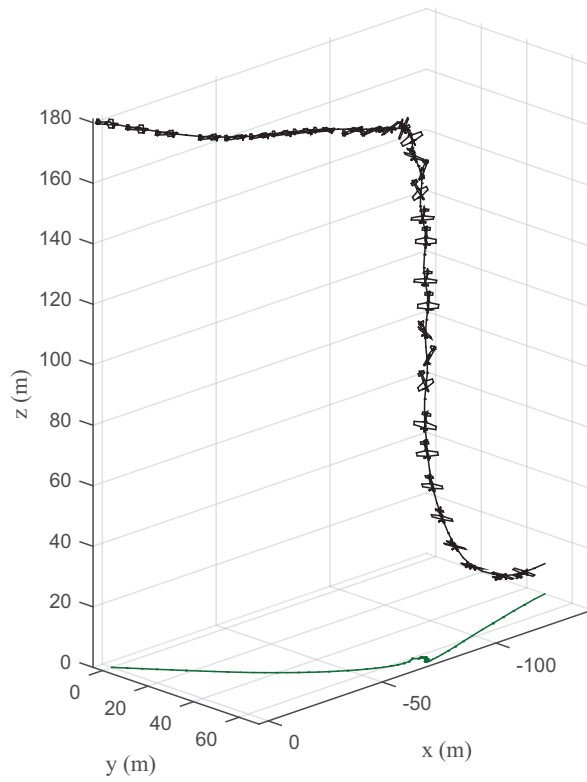


Figure 33. Trajectory of the aircraft during during spin with zero flap.

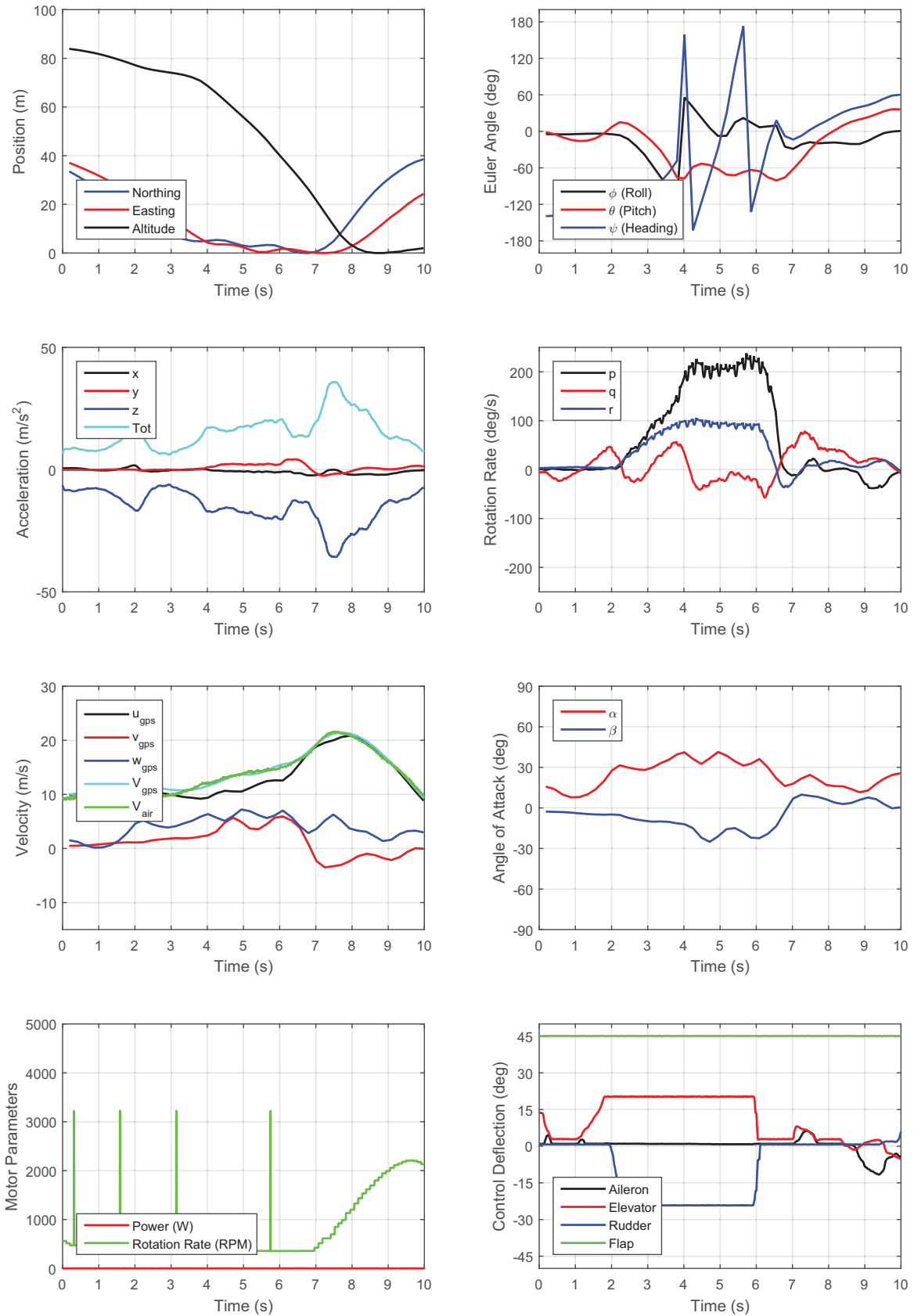


Figure 34. Time history of aircraft state during spin with full flap.

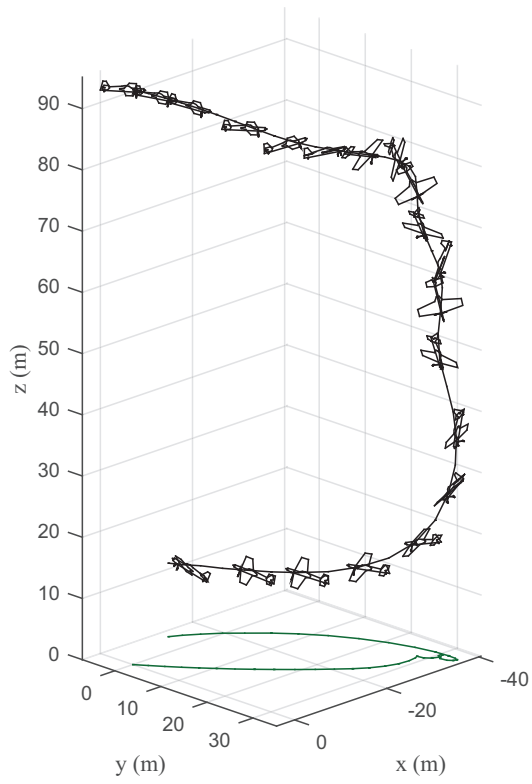


Figure 35. Trajectory of the aircraft during spin with full flap.

References

- ¹Lykins, R. and Keshmiri, S., "Modal Analysis of 1/3-Scale Yak-54 Aircraft Through Simulation and Flight Testing," AIAA Paper 2011-6443, AIAA Atmospheric Flight Mechanics Conference, Portland, Oregon, Aug. 2011.
- ²Johnson, B. and Lind, R., "Characterizing Wing Rock with Variations in Size and Configuration of Vertical Tail," *Journal of Aircraft*, Vol. 47, No. 2, 2010, pp. 567–576.
- ³Perry, J., Mohamed, A., Johnson, B., and Lind, R., "Estimating Angle of Attack and Sideslip Under High Dynamics on Small UAVs," Proceedings of the ION-GNSS Conference, Savannah, Georgia, 2008.
- ⁴Uhlig, D., Sareen, A., Sukumar, P., Rao, A. H., and Selig, M. S., "Determining Aerodynamic Characteristics of a Micro Air Vehicle Using Motion Tracking," AIAA Paper 2010-8416, AIAA Guidance, Navigation, and Control Conference, Toronto, Ontario, Canada, Aug. 2010.
- ⁵Dantsker, O. D. and Selig, M. S., "High Angle of Attack Flight of a Subscale Aerobatic Aircraft," AIAA Paper 2015-2568, AIAA Applied Aerodynamics Conference, Dallas, Texas, Jun. 2015.
- ⁶Mockli, M., *Guidance and Control for Aerobatic Maneuvers of an Unmanned Airplane*, Ph.D. thesis, ETH Zurich, Department of Mechanical and Process Engineering, 2006.
- ⁷Frank, A., McGrewy, J. S., Valentiz, M., Levinex, D., and How, J. P., "Hover, Transition, and Level Flight Control Design for a Single-Propeller Indoor Airplane," AIAA Paper 2007-6318, AIAA Guidance, Navigation, and Control Conference, Hilton Head, South Carolina, Aug. 2007.
- ⁸Johnson, E. N., Wu, A. D., Neidhoefer, J. C., Kannan, S. K., and Turbe, M. A., "Test Results of Autonomous Airplane Transitions Between Steady-Level and Hovering Flight," *Journal of Guidance, Control, and Dynamics*, Vol. 31, No. 2, 2008, pp. 358–370.
- ⁹Gaum, D. R., *Aggressive Flight Control Techniques for a Fixed-Wing Unmanned Aerial Vehicle*, Master's thesis, Stellenbosch University, Department of Electrical and Electronic Engineering, 2009.
- ¹⁰Bilodeau, P. R., Poulin, E., Gagnon, E., Wong, F., and Desbiens, A., "Control of a Hovering Mini Fixed Wing Aerial Vehicle," AIAA Paper 2009-5794, AIAA Guidance, Navigation and Control Conference, Chicago, Illinois, Aug. 2009.
- ¹¹Johnson, B. and Lind, R., "Trajectory Planning for Sensing Effectiveness with High Angle-of-Attack Flight Capability," AIAA Paper 2012-0276, AIAA Aerospace Sciences Meeting, Nashville, Tennessee, Jan. 2012.
- ¹²Jordan, T. L. and Bailey, R. M., "NASA Langley's AirSTAR Testbed: A Subscale Flight Test Capability for Flight Dynamics and Control System Experiments," AIAA Paper 2008-6660, AIAA Atmospheric Flight Mechanics Conference, Honolulu, HI, Aug. 2008.
- ¹³Ragheb, A. M., Dantsker, O. D., and Selig, M. S., "Stall/Spin Flight Testing with a Subscale Aerobatic Aircraft," AIAA Paper 2013-2806, AIAA Applied Aerodynamics Conference, San Diego, CA, Jun. 2013.
- ¹⁴Bunge, R. A., Savino, F. M., and Kroo, I. M., "Approaches to Automatic Stall/Spin Detection Based on Small-Scale UAV Flight Testing," AIAA Paper 2015-2235, AIAA Atmospheric Flight Mechanics Conference, Dallas, Texas, Jun. 2015.
- ¹⁵Dantsker, O. D., Ananda, G. K., and Selig, M. S., "GA-USTAR Phase 1: Development and Flight Testing of the Baseline Upset and Stall Research Aircraft," AIAA Paper 2017-4078, AIAA Applied Aerodynamics Conference, Denver, Colorado, June 2017.
- ¹⁶Risch, T., Cosentino, G., Regan, C., Kisska, M., and Princen, N., "X-48B Flight-Test Progress Overview," AIAA Paper 2009-934, AIAA Aerospace Sciences Meeting, Orlando, FL, Jan. 2009.
- ¹⁷Lundstrom, D. and Amadori, K., "Raven: A Subscale Radio Controlled Business Jet Demonstrator," International Congress on the Aeronautical Sciences Systems (ICUAS), Anchorage, Alaska, Sep. 2008.
- ¹⁸Regan, C. D. and Taylor, B. R., "mAEWing1: Design, Build, Test - Invited," AIAA Paper 2016-1747, AIAA Atmospheric Flight Mechanics Conference, San Diego, California, Jun. 2016.
- ¹⁹Regan, C. D., "mAEWing2: Conceptual Design and System Test," AIAA Paper 2017-1391, AIAA Atmospheric Flight Mechanics Conference, Grapevine, Texas, Jun. 2017.
- ²⁰Leong, H. I., Keshmiri, S., and Jager, R., "Evaluation of a COTS Autopilot and Avionics System for UAVs," AIAA Paper 2009-1963, AIAA Infotech@Aerospace, Seattle, Washington, April. 2009.
- ²¹Esposito, J. F. and Keshmiri, S., "Rapid Hardware Interfacing and Software Development for Embedded Devices Using Simulink," AIAA Paper 2010-3415, AIAA Infotech@Aerospace, Atlanta, Georgia, June 2010.
- ²²Garcia, G. and Keshmiri, S., "Integrated Kalman Filter for a Flight Control System with Redundant Measurements," AIAA Paper 2012-2499, AIAA Infotech@Aerospace, Garden Grove, California, June 2012.
- ²³National Aeronautics and Space Administration, "NASA Scientific and Technical Information (STI) Program," <https://www.sti.nasa.gov/>.
- ²⁴Group, U. A. A., "UIUC LSATs," https://m-selig.ae.illinois.edu/uiuc_satfaq.html.
- ²⁵UIUC Applied Aerodynamics Group, "UIUC Propeller Database," <http://m-selig.ae.illinois.edu/props/propDB.html>.
- ²⁶Jouannet, C., Lundstrom, D., Krus, P., da Silva, R. G. A., Catalano, F., and Greco, P., "Aerodynamic databased of a subscale demonstrator," AIAA Paper 2017-4075, AIAA Applied Aerodynamics Conference, Denver, Colorado, Jun 2017.
- ²⁷Al Volo LLC, "Al Volo: Flight Data Acquisition Systems," <http://www.alvolo.us>.
- ²⁸Xsens Technologies B.V., "XSens, MTi-G-700," <https://www.xsens.com/products/mti-g-700/>, Accessed Jan. 2016.
- ²⁹Dantsker, O. D., Vahora, M., Imtiaz, S., and Caccamo, M., "High Fidelity Moment of Inertia Testing of Unmanned Aircraft," AIAA Paper 2018-4219, AIAA Applied Aerodynamics Conference, Atlanta, Georgia, Jun. 2018.